Ergod. Th. & Dynam. Sys. (2021), **41**, 1397–1430
doi:10.1017/etds.2020.18

Dynamics and topological entropy of 1D Greenberg–Hastings cellular automata

M. KESSEBÖHMER, J. D. M. RADEMACHER and D. ULBRICH

Department 3: Mathematics, University of Bremen, Bibliothekstr. 5, 28359 Bremen, Germany
(e-mail: d.ulbrich@uni-bremen.de)

(*Received* 5 *March* 2019 *and accepted in revised form* 22 *January* 2020)

Abstract. In this paper we analyse the non-wandering set of one-dimensional Greenberg–Hastings cellular automaton models for excitable media with $e \geqslant 1$ excited and $r \geqslant 1$ refractory states and determine its (strictly positive) topological entropy. We show that it results from a Devaney chaotic closed invariant subset of the non-wandering set that consists of colliding and annihilating travelling waves, which is conjugate to a skew-product dynamical system of coupled shift dynamics. Moreover, we determine the remaining part of the non-wandering set explicitly as a Markov system with strictly less topological entropy that also scales differently for large e, r.

Key words: cellular automata, classical ergodic theory, symbolic dynamics, topological dynamics, low-dimensional dynamics
2020 Mathematics Subject Classification: 37B15, 37B20, 37B40 (Primary); 74J35 (Secondary)

1. *Introduction*

Following Greenberg, Hastings and Hassard [**6**], we consider a basic cellular automaton model of an excitable medium based on the alphabet

$$\mathcal{A} := \{0, 1, 2, \ldots, e, e+1, e+2, \ldots, e+r\},$$

of cardinality $\#\mathcal{A} := \mathrm{card}(\mathcal{A}) = \mathfrak{a} + 1$ for some positive integers e, r and $\mathfrak{a} := e + r$. Here, $E := \{1, 2, \ldots, e\}$ represents the *excited states*, $R := \{e+1, \ldots, \mathfrak{a}\}$ the set of *refractory states* and 0 is the *equilibrium rest state*. The special case $e = r = 1$ is the most studied case (see, in particular, [**5**]) even though the literature on this model is surprisingly scarce. However, the understanding of excitable media is of major importance in many different scientific contexts such as theoretical cardiology, neuroscience, chemistry, transition to turbulence, and surface catalysis, and it is a paradigm of nonlinear dynamics, self-organization and pattern formation [**9**, **11**]. Our main motivation stems from the problem of modelling strong interaction of localized nonlinear waves in spatially extended partial differential equations. On the one hand, only in simple cases can strong interaction be treated analytically rigorously. Even the major continuous models of excitable media, namely the FitzHugh–Nagumo-type systems, are not completely understood. On the other hand, in numerical simulation intricate spatio-temporal dynamics has been observed [**13**, **15**, **17**, **18**], but there seems to be no rigorous analysis of its complexity.

Unlike the special case $e = r = 1$, which has been treated in [**5**], we will show in this paper that in the case $\mathfrak{a} \geqslant 2$ the recurrent dynamics turns out to be in general much richer. We will provide a complete description of the recurrent dynamics: in addition to the pure pulse-annihilation dynamics, which is also present in the special case $e = r = 1$, there exists an intricate Markovian structure caused by stationary dislocations and defects. We complete our observation by showing that in terms of topological entropy the pulse-annihilation dynamics has a strictly higher complexity than the Markovian structure. It turns out that both parts of the dynamics scale differently with respect to an increase in the cardinality of excited and refractory states. We note that the topological entropy of cellular automata can have surprising properties and has been studied for several cases (see, for example, [**2**, **8**, **14**]), though to our knowledge no general results can be applied here. For $e = r = 1$ the entropy has been computed in [**5**] which serves as a guideline for the general case.

The cellular automaton model we study is a paradigmatic model of excitable media that captures many of the basic features. Let

$$X := \mathcal{A}^{\mathbb{Z}} = \{x = (\ldots, x_{-1}, x_0, x_1, \ldots) : x_k \in \mathcal{A} \text{ for all } k \in \mathbb{Z}\}$$

denote the full $\mathcal{A}$-shift [**12**]. Then $T : X \to X$ denotes the *cellular automaton* given by

$$T(\eta(x)) = \mathbf{E}(\eta(x)) + \mathbf{D}(\eta(x); \eta(x+1), \eta(x-1)),$$

where

$$\mathbf{E}(k) = k + 1,\ 1 \leqslant k \leqslant \mathfrak{a} - 1, \quad \text{and} \quad \mathbf{E}(\mathfrak{a}) = \mathbf{E}(0) = 0$$

and

$$\mathbf{D}(u; v_1, v_2) = \begin{cases} 1 & \text{if } u = 0 \text{ and } 1 \leqslant v_i \leqslant e \text{ for } i = 1 \text{ or } 2, \\ 0 & \text{otherwise.} \end{cases}$$

The function $\mathbf{E}$ can be thought of as the *reaction term* and $\mathbf{D}$ models the *interaction* between neighbouring cells. If a cell is not at rest, then it evolves according to the reaction term. If, in contrast, a cell is at rest then it becomes excited at level 1 if and only if at least one of its two neighbours is excited. We equip $\mathcal{A}$ with the discrete topology and X with the associated product topology which renders X compact and T continuous.

As the system is translation invariant both in space and time it allows for relative equilibria, in particular, travelling waves. The main building block of these are *pulses* of the form $x^* = (\ldots, 0, 0, 1, 2, \ldots, \mathfrak{a}, 0, 0, \ldots)$ and, spatially reflected, of the form x^{**} with $(x^{**})_k := (x^*)_{-k}$, $k \in \mathbb{Z}$. These pulses travel to the left and to the right, respectively. More specifically, if we define the left shift $\sigma_{\mathrm{L}} : X \to X$ by $(\sigma_{\mathrm{L}}(x))_k = x_{k+1}$, and the right shift, σ_R, analogously, then we have

$$T(x^*) = \sigma_L(x^*) \quad \text{and} \quad T(x^{**}) = \sigma_R(x^{**}).$$

The above observation remains valid also for left-moving (respectively, right-moving) *multi-pulses*, that is, for elements $x \in X$ given by arbitrary concatenations of the finite word $w^L := (1, 2 \ldots, \mathfrak{a})$ (also referred to as *local pulses*) and zeros (respectively, $w^R := (\mathfrak{a}, \mathfrak{a} - 1, \ldots, 1)$ and zeros). Due to the specific form of the coupling **D**, there is no dispersion, that is, the distances between local pulses remain fixed within each multi-pulse. Hence the restriction of T to the set of multi-pulses is conjugated to a left (respectively, right) shift-dynamical system. Further, this observation gives rise to the subsystem of counter-propagating semi-infinite multi-pulses. This invariant subsystem is determined by the key feature that pulses annihilate upon collision: in the simplest case, consider an initial datum $x := (\ldots, 0, 0, w^R, 0_{2\ell}, w^L, 0, 0, \ldots)$, where $0_{2\ell}$ denotes a block of zeros of length 2ℓ. Then T acts on x by decrementing ℓ so that $T^\ell(x) = (\ldots, 0, 0, w^R, w^L, 0, 0, \ldots)$ and $T^{\ell+\mathfrak{a}}(x) = (\ldots, 0, \ldots)$. We prove that the dynamics of counter-propagating semi-infinite multi-pulses with annihilation events constitutes a closed T-invariant Devaney chaotic subset $Z \subset X$ referred to as the *pulse-annihilation dynamics* (cf. Figure 4). Similarly to [**5**], we combinatorially determine the topological entropy of T restricted to Z to be twice the entropy of the (sub)shift dynamics on infinite pulse-trains. We show that on the corresponding subset Z_∞, on which pulse annihilation never ends, the dynamics of T is topologically conjugated to a skew-product dynamical system consisting of coupled shift dynamics, thus giving us a heuristic understanding of the concrete value of the topological entropy.

Since T is a continuous endomorphism of a compact metric space X, we know that the *non-wandering set* Ω of T (cf. Definition 4.1) carries the topological entropy of T, that is, $h(X, T) = h(\Omega, T|_\Omega)$. We shall show that the complexity of the dynamical system is already determined by further restricting to the pulse-annihilation dynamics $(Z, T|_Z)$.

The third author has shown in [**19**] that in the special case $e = r = 1$ the non-wandering set Ω, the pure pulse-annihilation system Z and the *eventual image* $Y := \bigcap_{n\in\mathbb{N}} T^n(X)$ all coincide. In contrast, for $\mathfrak{a} > 2$ both Ω and Z are strict subsets of Y. In order to determine the topological entropy of (X, T) we also have to study the complement of Z in the non-wandering set Ω, which, loosely speaking in terms of nonlinear wave phenomena, consists of stationary dislocations and defects; see Figure 5. This also leads to a complete understanding of the structure of the recurrent dynamics. For this we introduce transition graphs which determine the dynamics on $\Omega \setminus Z$; cf. Figure 7. An explicit formula allows us to compare the entropy of T restricted to Z with the entropy of T restricted to its complement in Ω. These explicit formulae allow us to study the limits as $e, r \to \infty$. On the one hand, asymptotically and after time-rescaling, the limiting entropy of the whole system is twice the topological entropy of the *full shift* over an alphabet with $\mathfrak{a}$ symbols. On the other hand, the limit of the restriction to $\Omega \setminus Z$ depends strongly on the difference of r and e.

This paper is organized as follows. In §2 we provide the basic setting and introduce the necessary notation. In §3 we focus on the pure pulse-annihilation subsystem and its skew-product representation. In the main section, §4, we give a detailed analysis of the non-wandering set and determine its topological entropy, including its asymptotics.

2. *Preliminaries and notation*

In this section we provide the topological set-up of our model and introduce some notational conventions as used in symbolic dynamics and throughout this paper.

2.1. *Topological setting.*

We recall that the topology on X is generated by the clopen *cylinder sets*, for $a_0, \ldots, a_n \in \mathcal{A}$, $n \in \mathbb{N}$ and $m \in \mathbb{Z}$,

$$[a_0, \ldots, a_n]_m := \{x \in X : x_m = a_0, \ldots, x_{m+n} = a_n\}.$$

The topological space X is compact and metrizable, and a metric inducing the topology is, for $x, y \in X$ for example, given by

$$d(x, y) = \begin{cases} 2^{-k} & \text{if } x \neq y \text{ and } k \text{ is maximal so that } x_{[-k,k]} = y_{[-k,k]}, \\ 0 & \text{if } x = y, \end{cases} \tag{1}$$

with the convention that if $x = y$ then $k = \infty$ and $2^{-\infty} = 0$, while if $x_0 \neq y_0$ then $k = -1$. See [**12**] for further details. Moreover, $T : X \to X$ is continuous with respect to the product topology.

The concept of *topological entropy* was first introduced for continuous self-maps of compact metric spaces by Adler, Konheim and McAndrews [**1**] and is a widely accepted measure of the complexity of a dynamical system. Bowen and Dinaburg [**3**, **4**] gave a definition for uniformly continuous maps on (not necessarily compact) metric spaces which coincides with the previous definition in the case of compactness. It was shown that the latter definition works for any continuous self-map whenever the metric on the space is totally bounded [**7**]. In this paper the topological entropy of T on X will be denoted by $h(X, T)$. Both the eventual image Y and the non-wandering set Ω determine the topological entropy, that is, $h(X, T) = h(Y, T|_Y) = h(\Omega, T|_\Omega)$ [**20**].

In this context, it is crucial to notice that Y is the set of all configurations $x \in X$ with $T^{-n}(x) \neq \varnothing$ for all $n \in \mathbb{N}$ and that $T : X \to X$ is not surjective: the preimage at a lattice site $j \in \mathbb{Z}$ is $T_j^{-1} : X \to \mathcal{A} \cup \{\{0, e+1\}\} \cup \varnothing$ with

$$T_j^{-1}(x) := \begin{cases} x_j - 1 & \text{if } x_j > 1, \\ 0 & \text{if } x_j = 1 \text{ and } x_{j-1} \in E+1 \text{ or } x_{j+1} \in E+1, \\ \mathfrak{a} & \text{if } x_j = 0 \text{ and } x_{j-1} \in E+1 \text{ or } x_{j+1} \in E+1, \\ \{0, \mathfrak{a}\} & \text{if } x_j = 0 \text{ and } x_{j\pm 1} \notin E+1, \\ \varnothing & \text{if } x_j = 1 \text{ and } x_{j\pm 1} \notin E+1, \end{cases} \tag{2}$$

where $E + 1 = \{a + 1 : a \in E\}$; note that $\mathcal{A} \setminus (E + 1) = \{0, 1, e + 2, \ldots, \mathfrak{a}\} = (R + 1) \cup \{1\}$ with addition mod $\mathfrak{a}$.

2.2. *Symbolic dynamics.*

We refer to $(a_1, a_2, \ldots, a_k) \in \mathcal{A}^k$ as a *block* (or *word*) over $\mathcal{A}$. The elements in X are also referred to as bi-infinite blocks. The length $|w|$ of a block w is the number of symbols it contains, that is, a k-block w is a block of length $|w| = k$. In particular, we use the notation $0_k := (0, \ldots, 0) \in \mathcal{A}^k$ for the k-block consisting only of zeros and 0_∞, $0_\infty^\pm$ for the (semi-)infinite zero blocks. Note that the action of T naturally carries over to the set of blocks.

For $i, j \in \mathbb{Z}$ with $i \leqslant j$, we denote the block of coordinates in x from position i to position j by $x_{[i,j]} = (x_i, x_{i+1}, \ldots, x_j)$. If $i > j$, $x_{[i,j]}$ is the empty block, denoted by $\varnothing$. For convenience, if $i, j \in \{\pm\infty\}$ and $p \in \mathbb{Z}$, we stick to this notation by setting $x_{[-\infty,p]} := (\ldots, x_{p-1}, x_p) \in \mathcal{A}^{\mathbb{Z}_{\leqslant p}}$, $x_{[p,\infty]} := (x_p, x_{p+1}, \ldots) \in \mathcal{A}^{\mathbb{Z}_{\geqslant p}}$ and $x_{[-\infty,\infty]} := x \in X$.

If w is a block, we say that w occurs in $x \in X$ (or that $x \in X$ contains w) if there are indices i and j such that $w = x_{[i,j]}$. A subblock of a block $w = (a_1, a_2, \ldots, a_k)$ is a block of the form $v = (a_i, a_{i+1}, \ldots, a_j)$ where $1 \leqslant i \leqslant j \leqslant k$, and we also say that v occurs in w or that w contains v and write $w = (a_1, a_2, \ldots, a_{i-1}, v, a_{j+1}, a_{j+2}, \ldots, a_k)$.

For finite blocks $w = (w_1, \ldots, w_m)$, $v = (v_1, \ldots, v_n)$ and a configuration $x \in [w, v]_{p-m+1} := [w_1, \ldots, w_m, v_1, \ldots, v_n]_{p-m+1}$, we use the notation

$$(w\ {}^{p}|v) = x_{[p-m+1,p+n]}$$

in order to specify the position $p \in \mathbb{Z}$ at which the two blocks are linked. In a slight abuse of this notation, if $w \in \bigcup_{q\in\mathbb{Z}} \mathcal{A}^{\mathbb{Z}_{\leqslant q}}$ is a left-infinite configuration and v is a finite block of length $n \in \mathbb{N}$, we write $x = (w\ {}^{p}|v)$ for the left-infinite configuration $x \in \mathcal{A}^{\mathbb{Z}_{\leqslant p+n}}$ with $x_{[-\infty,p]} = w$ and $x_{[p+1,p+n]} = v$ (and analogously for w and v being a finite block and a right-infinite configuration, respectively). If both w and v are semi-infinite, $x = (w\ {}^{p}|v)$ denotes the configuration $x \in X$ with $x_{[-\infty,p]} = w$ and $x_{[p+1,\infty]} = v$. In the same sense, we simply write

$$(w, v)$$

if the position is irrelevant.

To express the temporal dynamics of T, we use the transposed block notation

$$w^{\mathsf{T}} = (w_1, \ldots, w_n)^{\mathsf{T}} := \begin{pmatrix} w_n \\ \vdots \\ w_1 \end{pmatrix}.$$

A configuration $x \in X$ or a block $\omega = x_{[i,j]}$ occurring in x is n-periodic if $n \geqslant 1$ is the smallest integer such that $T^n(x) = x$, or $(T^n(x))_{[i,j]} = \omega$, respectively.

In the sequel, we need some notion of 'distance' between states $a, b \in \mathcal{A}$. To this end, we make the convention to consider $\mathcal{A}$ as the group $(\mathbb{Z}/(\mathfrak{a}+1)\mathbb{Z}, +)$, while inequalities involving elements in $\mathcal{A}$ are meant with respect to $\mathbb{Z}$.

Definition 2.1. For $a, b \in \mathcal{A}$, let $\mathcal{A} \ni s(a, b) := b - a$ be the *step size from a to b*.

For illustration, it is convenient to think of the corresponding alphabet

$$\widehat{\mathcal{A}} := \{\widehat{a} = e^{i\psi(a)} : a \in \mathcal{A}\} = \widehat{E} \cup \widehat{R}, \quad \psi(a) := 2\pi a/(\mathfrak{a}+1), \tag{3}$$

on $\{x \in \mathbb{C} : |x| = 1\}$; cf. Figure 1.

3. *The pulse-collision subsystem*

We first consider the aforementioned invariant subsystem for which we can compute the topological entropy explicitly and infer other features of the dynamics. This will already give a lower estimate for the topological entropy and complexity of the whole system. This subsystem depends on $\mathfrak{a}$ only and thus is a lower complexity bound independent of the order of e and r.

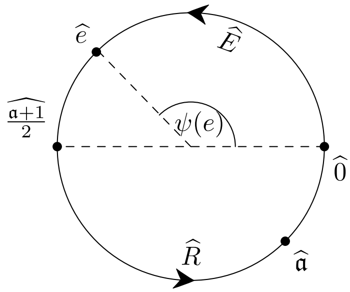

FIGURE 1. Illustration of $\widehat{\mathcal{A}}$ for the particular case $r = e + 1$.

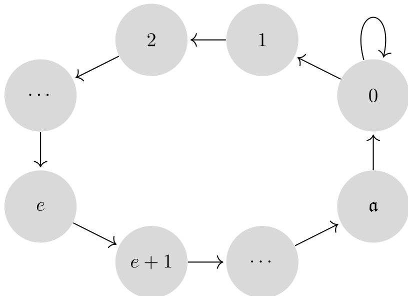

$$\begin{array}{c} \\ 0 \\ 1 \\ \vdots \\ \mathfrak{a}-1 \\ \mathfrak{a} \end{array} \begin{array}{c} \begin{array}{ccccc} 0 & 1 & 2 & \dots & \mathfrak{a} \end{array} \\ \begin{bmatrix} 1 & 1 & 0 & \dots & 0 \\ 0 & 0 & 1 & \dots & 0 \\ \vdots & \vdots & \vdots & \ddots & \vdots \\ 0 & 0 & 0 & \dots & 1 \\ 1 & 0 & 0 & \dots & 0 \end{bmatrix} \end{array} = A$$

FIGURE 2. Transition graph for the one-sided subshift defining the pulse system.

The set of multi-pulses and infinite wavetrains mentioned in the introduction forms a subshift constructed by the transition graph plotted in Figure 2 (left): adjacent block entries differ by one or are both zero, that is, $s(x_i, x_{i+1}) \in \{\mathrm{sgn}(x_i), 1\}$ or $s(x_{i+1}, x_i) \in \{\mathrm{sgn}(x_{i+1}), 1\}$. The transition matrix $A \in \{(a_{i,j})_{i,j=1}^{\mathfrak{a}+1} : a_{i,j} \in \{0, 1\}\}$ corresponding to this graph is shown in Figure 2 (right).

Accordingly, we define sets of right- and left-moving infinite multi-pulse-type solutions,

$$S_{\mathrm{R}} := \{x \in \mathcal{A}^{\mathbb{Z}} : a_{x_i, x_{i-1}} = 1,\ i \in \mathbb{Z}\}, \quad S_{\mathrm{L}} := \{x \in \mathcal{A}^{\mathbb{Z}} : a_{x_i, x_{i+1}} = 1,\ i \in \mathbb{Z}\},$$

their semi-infinite analogues,

$$S_{\mathrm{R}}^{-} := \bigcup_{p \in \mathbb{Z}} S_{\mathrm{R},p}^{-}, \quad S_{\mathrm{R},p}^{-} := \{x \in \mathcal{A}^{\mathbb{Z}_{\le p}} : a_{x_i, x_{i-1}} = 1\},$$
$$S_{\mathrm{L}}^{+} := \bigcup_{p \in \mathbb{Z}} S_{\mathrm{L},p}^{+}, \quad S_{\mathrm{L},p}^{+} := \{x \in \mathcal{A}^{\mathbb{Z}_{\ge p}} : a_{x_i, x_{i+1}} = 1\},$$

and infinite configurations composed of semi-infinite counter-propagating parts,

$$S_{\mathrm{L}}^{\mathrm{R}} := \bigcup_{p \in \mathbb{Z}} \{(x^{\mathrm{R}\ p} | x^{\mathrm{L}}) \in S_{\mathrm{R},p}^{-} \times \mathrm{S}_{\mathrm{L},p+1}^{+}\} \setminus (S_{\mathrm{R}} \cup S_{\mathrm{L}}).$$

In the definition of $S_{\mathrm{L}}^{\mathrm{R}}$ we have identified pairs in $S_{\mathrm{R},p}^{-} \times S_{\mathrm{L},p+1}^{+}$ with configurations in X by gluing these together at position p. Conversely, for given $x \in S_{\mathrm{L}}^{\mathrm{R}}$ this position is not unique, but there are only finitely many options $p \in \mathbb{Z}$ such that $(x_{[-\infty,p]}, x_{[p+1,\infty]}) \in S_{\mathrm{L}}^{\mathrm{R}}$ since $x \notin S_{\mathrm{R}} \cup S_{\mathrm{L}}$. This motivates the following notion.

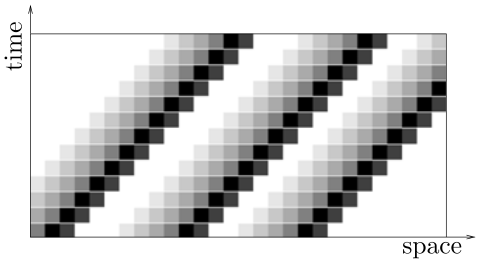

FIGURE 3. Snapshot of T acting on S_{R} as right shift σ_{R}.

Definition 3.1. For $x \in S_{\mathrm{L}}^{\mathrm{R}} \cup S_{\mathrm{R}} \cup S_{\mathrm{L}}$ we call $p \in \overline{\mathbb{Z}} := \mathbb{Z} \cup \{\pm\infty\}$ a separating position if $(x_{[-\infty,p]}, x_{[p+1,\infty]}) \in S_{\mathrm{L}}^{\mathrm{R}}$ or either $x_{[-\infty,p]} \in S_{\mathrm{R}}$ with $p = \infty$ or $x_{[p,\infty]} \in S_{\mathrm{L}}$ with $p = -\infty$. We denote the set of separating positions of x by $I_{\mathrm{sp}}(x)$, or simply by I_{sp} if x is clear from the context.

Note that $\#I_{\mathrm{sp}} = 1$ for $x \in S_{\mathrm{R}} \cup S_{\mathrm{L}}$ and $\#I_{\mathrm{sp}} < \infty$ for $x \in S_{\mathrm{L}}^{\mathrm{R}}$. T acts as the right shift σ_{R}, $(\sigma_{\mathrm{R}}(x))_{j+1} = x_j$, on S_{R} and on S_{L} as the left shift σ_{L}, so that S_{R}, S_{L} form invariant subsets of X; cf. Figure 3. Conversely, T acts as a shift on such configurations only. On finite blocks of type S_{R} or S_{L} the map T acts on $x_{[j_-+1,j_+-1]}$ as the corresponding shift, and thus locally in space. On S_{R}^- and S_{L}^+ the shifts are denoted by $\sigma_{\mathrm{R},-}$, $\sigma_{\mathrm{L},+}$, respectively.

We now define the key notion of this section.

Definition 3.2. The pulse-collision subsystem $Z \subset S_{\mathrm{L}} \cup S_{\mathrm{R}} \cup S_{\mathrm{L}}^{\mathrm{R}}$ is the set of $x \in X$ with either $x \in S_{\mathrm{R}} \cup S_{\mathrm{L}}$ or $x \in S_{\mathrm{L}}^{\mathrm{R}}$ such that, for $p = \max I_{\mathrm{sp}}(x)$, we have $x_{p+1} = x_p$ or $(x_{[-\infty,p]}, x_{[p,\infty]}) \in S_{\mathrm{L}}^{\mathrm{R}}$. Let $Z_\infty \subset Z \cap S_{\mathrm{L}}^{\mathrm{R}}$ be the subset of configurations $x \in S_{\mathrm{L}}^{\mathrm{R}}$ for which $x_{[-\infty,k]} \neq 0_\infty^-$, $x_{[k,\infty]} \neq 0_\infty^+$ for all $k \in \mathbb{Z}$.

As will be discussed more in the sequel, Z consists of configurations which are either purely left- or right-moving under the dynamics of T, or sequences of local pulses w^{L} (leftwards) and w^{R} (rightwards) glued at one position, which annihilate each other in time. That is, the dynamics on Z consists entirely of pulse dynamics and pulse annihilation; cf. Figure 4. The set $Z_\infty \subset S_{\mathrm{L}}^{\mathrm{R}}$ captures the configurations for which the collision and annihilation never ends. More specifically, for $x \in Z$ with separating position $p \in \mathbb{Z}$, there is $(x^{\mathrm{R}}, x^{\mathrm{L}}) \in S_{\mathrm{L}}^{\mathrm{R}}$ such that $x = (x^{\mathrm{R}}\ {}^p|x^{\mathrm{L}})$ and some $\tilde{x} \in T^{-n}(x) \in S_{\mathrm{L}}^{\mathrm{R}}$ for some minimal $n \in \mathbb{N}_0$ such that $\tilde{x}$ is of pre-collision type, that is, $\tilde{x} = (\tilde{x}^{\mathrm{R}}, 0_\ell, \tilde{x}^{\mathrm{L}})$ with $\tilde{x}^{\mathrm{R}} = (\ldots, 2, 1)$, $\tilde{x}^{\mathrm{L}} = (1, 2, \ldots)$ and separating interval $I_{\mathrm{sp}} = [p_-, p_+]$ with $\tilde{x}_{[p_-,p_+]} = (1, 0_\ell)$. Recall the dynamics of iterating T for even $\ell = 2\ell'$ decrements ℓ' until $\ell = 0$, namely,

$$T^j(x) = (x^{\mathrm{R}}, 0_{2(\ell'-j)}, x^{\mathrm{L}}), \quad x_{[-\infty,p_-]} = x^{\mathrm{R}}, \quad j = 0, 1, \ldots, \ell'.$$

After this the annihilation takes place for $T^{\ell'+j}(x)$, $j = 0, 1, \ldots, \mathfrak{a}$, which is characterized by a unique and constant separating position p and by $x_p = x_{p+1}$. These values are incremented until both are $\mathfrak{a}$ and the next time step leads to $x_p = x_{p+1} = 0$ so the pulses have annihilated each other.

For odd ℓ, the annihilation starts via

$$T(\ldots, 2, 1, 0, 1, 2, \ldots) = (\ldots, 3, 2, 1, 2, 3, \ldots),$$

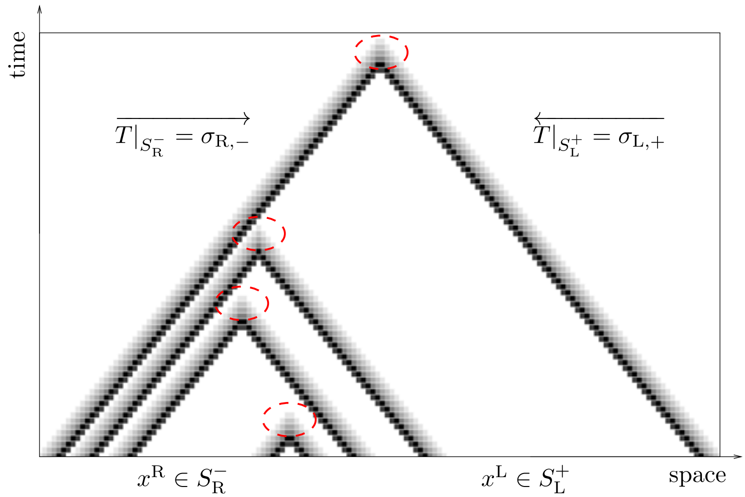

FIGURE 4. Space–time plot of Greenberg–Hastings cellular automaton simulation of $x = (x^R, x^L) \in S_L^R$. Marked is a sequence of four pulse annihilation events for $e = 2$ and $r = 4$; the rest state is shown in white, the grey levels increase in order $\mathfrak{a}, \mathfrak{a} - 1, \ldots, e + 1, 1, \ldots, e$.

where dots denote some continuation in S_R, S_L, respectively. The central block $(1, 0, 1)$ in the preimage determines the separating positions, lying either at the leftmost 1 or at the 0, so, in contrast to annihilation for even ℓ, here we have two separating positions, $I_{sp} = [p, p + 1]$, where $p + 1$ lies at the centre of the block $(1, 0, 1)$ in the preimage. Further iteration yields the annihilation analogous to the even case, except that there are two separating positions. Notably, at collision (i.e. when there are no zeros at separating positions) and during annihilation we have $x_{[p,\infty]}, x_{[p+1,\infty]} \in S_L$.

Remark 3.3. In summary, the pre-collision-type configuration

$$x = (x^R, 0_\ell, x^L) \text{ with } (x^R, x^L) = (\ldots, 2, 1, 1, 2, \ldots) \in S_L^R$$

has $I_{sp} = [p_-, p_+]$, and $x_{[p_-,p_+]} = (1, 0_\ell)$. For even $\ell > 0$, the number of separating positions is odd and the collision is characterized by a block $(2, 1\ {}^p|1, 2)$ with unique separating position p (i.e. $\#I_{sp} = 1$). This remains the unique separating position for $\mathfrak{a}$ time steps. For odd ℓ, the number of separating positions is even and pulse collision occurs at a block $(2, 1, 2)$ which yields two separating positions, $\#I_{sp} = 2$, also during annihilation.

In the cases $x^R \equiv 0$ or $x^L \equiv 0$ and more generally for $x \in S_R \cup S_L$ the separating positions also form an interval $I_{sp} = [p_-, p_+]$, with $p_+ = \infty$ or $p_- = -\infty$, or $I_{sp} = [\pm\infty]$ for one sign.

LEMMA 3.4.
(i) *$T(S_R) = S_R$, $T(S_L) = S_L$, and $T|_{S_R} = \sigma_R|_{S_R}$, $T|_{S_L} = \sigma_L|_{S_L}$ are invertible.*
(ii) *$T(Z) = Z \subset Y$, $T(Z_\infty) = Z_\infty$,*
(iii) *Let $x \in Z$. If $\#I_{sp} = 1$ or $x_{p+1} \neq 0$ with $I_{sp} = [p, p + 1]$, then x has a unique preimage under T in Z. Otherwise there are $\#I_{sp}$ possible preimages in Z.*
(iv) *Z is closed (hence compact) and Z_∞ is not closed with closure $\overline{Z_\infty} = Z$.*

https://doi.org/10.1017/etds.2020.18 Published online by Cambridge University Press

Proof. (i) As noted above, S_{R} and S_{L} are naturally forward invariant under T. For $x \in S_{\mathrm{R}}$, there is a unique preimage in S_{R} being the left or right shift, respectively. More precisely, each 1 lies in a block (2, 1, 0) and each 0 lies in the centre of a block (0, 0, 0) or (1, 0, 0) with unique preimage in S_{R} being 0, or it lies in a block $(0, 0, \mathfrak{a})$ with unique preimage in S_{R} being $\mathfrak{a}$. Analogously. this holds for $T|_{S_{\mathrm{L}}} : S_{\mathrm{L}} \to S_{\mathrm{L}}$.

(ii) The argument in (i) and the annihilation procedure discussed above show that the image of Z lies in Z, and also that each point in Z has a preimage in Z, which means $Z \subset Y$. Likewise for Z_∞.

(iii) The case $\#I_{\mathrm{sp}} = 1$ implies either $x \in S_{\mathrm{R}} \cup S_{\mathrm{L}}$, in which case the preimage in Z is unique as in item (i), or otherwise $x = (x^{\mathrm{R}}, x^{\mathrm{L}}) \in S^{\mathrm{R}}_{\mathrm{L}}, x^{\mathrm{L}} \in S_{\mathrm{L}}$, as in Remark 3.3 for $\ell = 0$ with $x_p = x_{p+1} > 0$ and the unique preimage in Z is $(x^{\mathrm{R}}, 0, 0, x^{\mathrm{L}})$ with zeros at positions p and $p + 1$. The case of two separating positions corresponds to the annihilation from odd ℓ and again $x = (x^{\mathrm{R}}, x^{\mathrm{L}})$ with $x_p = x_{p+1} + 1 > 1$ by assumption so that the unique preimage in Z is $(x^{\mathrm{R}}, x_p - 1, x^{\mathrm{L}})$ with $x_p - 1$ at position p.

Finally, if $I_{\mathrm{sp}} = [p_-, p_+]$ with $p_+ - p_- > 2$ then $x_{[p_-,p_+]} = (1, 0_\ell)$ for $\ell = p_+ - p_- - 1$ (cf. Remark 3.3) and $x = (x^{\mathrm{R}}, 0_\ell, x^{\mathrm{L}})$ with $x_{[-\infty,p_-]} = x^{\mathrm{R}}$. The possible preimages are $x^0 = (x^{\mathrm{R}}, 0_{\ell+2}, x^{\mathrm{L}})$ and $x^j = (x^{\mathrm{R}}, 0_j, \mathfrak{a}, 0_{\ell-j+1}, x^{\mathrm{L}})$ with $x^0_{[-\infty,p_--1]} = x^{\mathrm{R}}$ and $j = 1, \ldots, \ell$, which makes $\#I_{\mathrm{sp}} = \ell + 1$.

(iv) By construction of elements in Z it contains limits of converging sequences. Since such limits of a sequence in Z_∞ may be, for example, the zero sequence, Z_∞ is not closed. However, any point in Z can be approximated in the cylinder topology with a sequence in Z_∞ by replacing the infinite tails with tails of elements from Z_∞. □

3.1. *Topological entropy on Z and its asymptotics.* We determine the topological entropy of $(Z, T|_Z)$. The proof is an adaption and more complete exposition of the technique in [**5**] for the case $e = r = 1$, which is special as $Y = Z$, which has been shown by the third author in [**19**], that is, eventual image and pulse-collision subsystem coincide in this case only. We remark that it is purely a combinatorial counting argument of space–time windows and in this sense independent of the topology.

PROPOSITION 3.5. *The topological entropy of T restricted to Z is given by $h(Z, T|_Z) = 2 \ln \rho_{\mathfrak{a}}$, where $\rho_{\mathfrak{a}}$ denotes the largest eigenvalue of A, which is the positive real root of $\lambda^{\mathfrak{a}+1} - \lambda^{\mathfrak{a}} - 1$. In particular, $h(X, T) \geqslant 2 \ln \rho_{\mathfrak{a}}$.*

Proof. We determine a substitution for Z by (essentially) replacing each pulse travelling right (left) with an 'r' ('ℓ') symbol at the $\mathfrak{a}$ state and all other states by zeros; thus between two rs and between two ℓs there are at least $\mathfrak{a}$ zeros. Specifically, let $Z' \subset \{0, r, \ell\}^{\mathbb{Z}}$ be the set of configurations z for which there exists some $p \in \mathbb{Z} \cup \{\pm\infty\}$ such that:

(1) $z_i \in \{0, r\}$ for all $i \leqslant p$, and $|i - j| > \mathfrak{a}$ for all $i, j \in \mathbb{Z}_{\leqslant p}, i \neq j : z_i = z_j = r$;

(2) $z_i \in \{0, \ell\}$ for all $i > p$, and $|i - j| > \mathfrak{a}$ for all $i, j \in \mathbb{Z}_{>p}, i \neq j : z_i = z_j = \ell$.

On Z' we define $T' \colon Z' \to Z'$ by shifting rs to the right, ℓs to the left and letting rs and ℓs annihilate each other upon collision, that is, $T'((z^{\mathrm{R}}, r, \ell, z^{\mathrm{L}})) = (z^{\mathrm{R}}, z^{\mathrm{L}})$ and $T'((z^{\mathrm{R}}, r, 0, \ell, z^{\mathrm{L}})) = (z^{\mathrm{R}}, 0, z^{\mathrm{L}})$ (here $z^{\mathrm{R}}, z^{\mathrm{L}}$ do not have r, ℓ at the right- or leftmost

https://doi.org/10.1017/etds.2020.18 Published online by Cambridge University Press

position, respectively). We define a map $U: Z \to Z'$ by

$$(U(x))_i := \begin{cases} r & \text{if } x_i = \mathfrak{a} \text{ and } x_{i+1} \in \{\mathfrak{a}-1, \mathfrak{a}\}, \\ \ell & \text{if } x_i = \mathfrak{a} \text{ and } x_{i-1} \in \{\mathfrak{a}-1, \mathfrak{a}\}, \\ 0 & \text{otherwise}, \end{cases} \tag{4}$$

which is surjective and satisfies $U \circ T|_Z = T' \circ U$. From a topological viewpoint, Z' equipped with the cylinder topology renders U continuous, that is, (Z', T') is a topological factor of $(Z, T|_Z)$ so that $h(Z', T') \leqslant h(Z, T|_Z)$.

However, U is not a bijection since $(0, \mathfrak{a}, 0)$ (the last stage of an odd annihilation) is mapped to $(0, 0, 0)$, as is $(0, 0, 0)$ itself; the issue is that $\mathfrak{a}$ should be mapped to r and ℓ simultaneously for consistency with T. Hence, for $z \in Z'$ with a block $(r, 0_{2\mathfrak{a}+k+3}, \ell)$ (note there can be at most one such block) we have $\#U^{-1}(z) = k$, and infinitely many preimages occur for z with semi-infinite zero block. Nevertheless, U has a unique inverse except in the case of a block $(0, 0, 0)$.

We next follow [**5**] in order to compute $h(Z', T') = 2 \ln \rho_{\mathfrak{a}}$ and define

$$c_q(z'_{[k_1,k_2]}) := \#\{z'(k) = q : k \in [k_1, k_2]\} \tag{5}$$

to count the number of symbols q in the block $z'_{[k_1,k_2]}$ and

$$\gamma_{g,n}(q) := \#\{z'_{[0,n-1]} : z' \in Z', c_q(z'_{[0,n-1]}) = g\} \tag{6}$$

to be the number of ways of putting down g symbols q on an integer interval of length n with at least $\mathfrak{a}$ zeros in between. Moreover, let

$$\gamma_n(q) := \sum_{g=0}^{n} \gamma_{g,n}(q), \tag{7}$$

which is the number of ways of putting any number of symbols q on an integer interval of length n with at least $\mathfrak{a}$ zeros in between. This is the number of allowed words of length n of the pure left or right subshifts, hence (cf. [**12**])

$$\limsup_{n\to\infty} \frac{\gamma_n(\ell)}{n} = \ln \rho_{\mathfrak{a}}, \tag{8}$$

where $\rho_{\mathfrak{a}}$ is the largest eigenvalue of the matrix A; cf. Figure 2. Finally, for a space–time window of symbols, $W_{m,n} := \{0, r, l\}^{[-m,m]\times[0,n-1]}$, let

$$\Gamma_{n,m} := \operatorname{card}\{W_{m,n} : \exists z' \in Z' : W_{m,n} = (z', T'z', \ldots, (T')^{n-1}z')_{[-m,m]}\}, \tag{9}$$

where the block formation is meant rowwise. This is the number of space–time windows $W_{m,n}$ that can be extended in space to be in an orbit of T' on Z'. The topological entropy of $h(Z', T')$ can then equivalently be defined as (cf. [**5, 19**])

$$h(Z', T') := \sup_m \limsup_{n\to\infty} \frac{1}{n} \ln \Gamma_{m,n}. \tag{10}$$

We first show that $h(Z', T') \geqslant 2 \ln \rho_{\mathfrak{a}}$. To this end, we construct a sufficiently rich set of initial data in Z' to generate different $W_{m,n}$. Let $t > 0$ be some integer and $n = t(m + \mathfrak{a})$.

https://doi.org/10.1017/etds.2020.18 Published online by Cambridge University Press

Consider the blocks $z'_{[-n,n]}$ for initial data of the form $z' = (z^{\mathrm{R}}, 0, z^{\mathrm{L}}) \in Z'$, where z^{R} is a semi-infinite configuration of rs and 0s with at least $\mathfrak{a}$ 0s between two rs, and similarly for z^{L}. Let h_j, for $\pm j = 1, \ldots, t$, be blocks of length m and consider

$$z^{\mathrm{L}}_{[1,n]} = (h_1, 0_{\mathfrak{a}}, h_2, 0_{\mathfrak{a}} \ldots, h_t, 0_{\mathfrak{a}}),$$
$$z^{\mathrm{R}}_{[-n,-1]} = (0_{\mathfrak{a}}, h_{-t}, 0_{\mathfrak{a}}, h_{-t+1}, \ldots, h_{-2}, 0_{\mathfrak{a}}, h_{-1}),$$

with $c_l(h_j) = c_r(h_{-j})$ for each $j = 1, \ldots, t$. By construction, different such initial data differ at some point in $W_{m,n}$ and hence the number of these initial configurations is a lower bound for the total number of different space–time windows. Since for each j we can independently assign symbols in $h_{\pm j}$, for each j the number of these pairs with g non-zero symbols is $\gamma_{g,m}(r) \cdot \gamma_{g,m}(\ell) = \gamma_{g,m}(r)^2$. Since each subblock can be independently assigned symbols, the total number of such initial data is

$$\left(\sum_{g=0}^{m} \gamma_{g,m}(\ell)^2\right)^t \tag{11}$$

so that

$$h(Z', T') \geqslant \frac{1}{t(m+2)} \ln\left(\sum_{g=0}^{m} \gamma_{g,m}(\ell)^2\right)^t = \frac{1}{m+2} \sum_{g=0}^{m} \gamma_{g,m}(\ell)^2. \tag{12}$$

Finally, we use the fact that for any $\varepsilon > 0$ there exists an m such that $(1/(m+2)) \sum_{g=0}^{m} \gamma_{g,m}(\ell)^2 \geqslant \ln \rho_{\mathfrak{a}} - \varepsilon$ and thus $h(Z', T') \geqslant 2 \ln \rho_{\mathfrak{a}} - \varepsilon$ for any $\varepsilon > 0$ so that $h(Z', T') \geqslant 2 \ln \rho_{\mathfrak{a}}$.

In order to prove $h(Z', T') \leqslant 2 \ln \rho_{\mathfrak{a}}$, note that $\Gamma_{m,n}$ is at most the number of initial data $z' \in Z'$ for which a change in z' has a chance of resulting in a change in $W_{m,n}$. Since the speed of propagation is one, it follows that only the blocks $z'_{[-m-n+1,m+n-1]}$ can have an impact on $W_{m,n}$. Moreover, any $\ell \in z'_{[-m-n+1,-m]}$ has no impact on $W_{m,n}$ since it is moving to the left. Likewise, any r in $z'_{[m,m+n-1]}$ has no impact on $W_{m,n}$. Hence $\Gamma_{m,n}$ is less than or equal the number N of configurations $z' \in Z'$ with $c_\ell(z'_{[-m-n+1,-m]}) = 0 = c_r(z'_{[m,m+n-1]})$. Due to these restrictions on $z'_{[-m-n+1,m]}$ and $z'_{[-m,m+n-1]}$, we have that $N \leqslant \gamma_{2m+n}(r)\gamma_{2m+n}(\ell) = \gamma_{2m+n}(\ell)^2$, that is,

$$h(Z', T') \leqslant \sup_m \limsup_{n\to\infty} \frac{1}{n} \ln \gamma_{2m+n}(\ell)^2 = 2 \ln \rho_{\mathfrak{a}}. \tag{13}$$

Since U is not finite-to-one Bowen's inequality does not directly imply $h(T, Z) \leqslant 2 \ln \rho_{\mathfrak{a}}$ as the fibre entropy is not *a priori* zero (cf. [**3**]). Since $\mathfrak{a}$ is mapped to 0 under T, the previous counting misses precisely the options to replace 0 with $\mathfrak{a}$ within a zero block in $W_{n,m}$. However, the preimage in Z of $(0, \mathfrak{a}, 0)$ under T is $(\mathfrak{a}, \mathfrak{a}-1, \mathfrak{a})$, on which U is bijective. Hence, the only options for $W_{m,n}$ that have not been accounted for in $\Gamma_{m,n}$ concern the bottom row of $W_{m,n}$. Since these are at most $2m$, this extra contribution vanishes in the limit as $\ln(\gamma_{2m+n}(\ell)^2 + 2m) \leqslant \ln(\gamma_{2m+n}(\ell)^2) + \ln(2m)$, that is, it carries zero entropy. This concludes the proof. □

Remark 3.6. In this proof the largest growth rate of different space–time windows, and thus the topological entropy, stems from counting enduring annihilations, that is, elements in the set Z_∞. In this sense the topological entropy is generated by Z_∞.

Let us study what happens with the topological entropy as $\mathfrak{a}$ increases. Despite the increasing number of states, the system's complexity, measured by the entropy, actually decreases since the rigid reaction dynamics of incremental steps takes more time.

LEMMA 3.7. *The largest positive root ρ_t of the polynomial $f_t(\lambda) := \lambda^{t+1} - \lambda^t - 1$ is strictly greater than one and we have $\rho_t - 1 \sim (\ln t)/t$ as $t \to \infty$.*

Proof. By Descartes' rule of signs, the polynomial f_t has exactly one positive (simple) root ρ_t. Moreover, $\rho_t > 1$ since $f_t(\lambda) < 0$ for $\lambda \in [0, 1]$. Since $(1 + (\ln t)/t)^t = e^{t \ln(1+(\ln t)/t)} \sim e^{\ln t} = t$ as $t \to \infty$, we have

$$f_t\left(1 + \frac{\ln(t)}{t}\right) = \left(1 + \frac{\ln(t)}{t}\right)^t \frac{\ln(t)}{t} - 1 \sim \ln(t) - 1 > 0, \quad t \to \infty.$$

Consequently, $\rho_t \in (1, 1 + (\ln(t))/t)$ for large values of t and $\lim_{t\to\infty} \rho_t = 1$.

Now, since $f_t(1 + \xi_t) = 0$ if and only if $(1 + \xi_t)^t \xi_t = e^{t \ln(1+\xi_t)} \xi_t = 1$ and $e^{t \ln(1+\xi_t)} \sim e^{t\xi_t}$, we get $t\xi_t e^{t\xi_t} \sim t$ as $t \to \infty$. Applying the Lambert function W and using its large-argument approximation, we find that $t\xi_t \sim W(t) \sim \ln(t)$ as $t \to \infty$, which concludes the proof. □

However, viewing $\mathfrak{a}$ as a discretization in space, the rescaling of time that preserves velocities is linear in $\mathfrak{a}$; the associated entropy then increases proportionally with $\log \mathfrak{a}$. More precisely we have the following corollary.

COROLLARY 3.8. *The topological entropy of T on Z for a time-rescaling $\alpha : \mathbb{N} \to \mathbb{N}$ satisfies $h(Z, T^{\alpha(\mathfrak{a})}) = 2 \ln(\rho_{\mathfrak{a}}^{\alpha(\mathfrak{a})}) \sim 2\alpha(\mathfrak{a})(\ln \mathfrak{a})/\mathfrak{a}$ as $\mathfrak{a} \to \infty$. In particular, for $\alpha : n \mapsto n$, the topological entropy asymptotically doubles the topological entropy of the full $\mathfrak{a}$-shift.*

Proof. This is a direct consequence of Lemma 3.7. □

Remark 3.9. The restriction on $\Omega \setminus Z$ scales differently as the cardinality of excited and refractory states increases; cf. Remark 4.28.

3.2. *Waiting times, coherent structures and chaos.* Since the dynamics on Z_∞ consists entirely of pulses moving towards each other until collision, it is natural to encode this in terms of waiting and annihilation times. Each $x \in Z_\infty$ away from pulse annihilation and collision has the form

$$(\ldots, 0_{k_j}, w^{\mathrm{R}}, 0_{k_{j+1}}, \ldots, w^{\mathrm{R}}, 0_{k_0}, w^{\mathrm{L}}, 0_{k_1}, w^{\mathrm{L}}, \ldots)$$

for a sequence of *waiting times* $(k_j)_{j\in\mathbb{Z}} \subset \mathbb{N}$ between the end of an annihilation and the next collision. Recall that a collision occurs precisely when $I_{\mathrm{sp}}(x) = [p_-, p_+]$, $1 \leqslant p_+ - p_- \leqslant 2$ and $x_{p_-} = x_{p_+} = 1$; the end of the collision is reached one iteration step after $x_{p_-} = x_{p_+} = \mathfrak{a}$.

Clearly, $k_0 + 1 = \#I_{\mathrm{sp}}(x)$, and if $k_0 \geqslant 1$ then the position of the initial collision, $c_0 \in \mathbb{Z}$, under the dynamics of T is at the lattice site of the (left-)centre $c_0 = \lfloor (p_- + p_+)/2 \rfloor$ of $I_{\mathrm{sp}}(x) = [p_-, p_+]$, and this happens at time $t_0 = \lfloor k_0/2 \rfloor$. Otherwise, the initial condition lies in an annihilation event in which case c_0 is as in the previous case, but $t_0 = 1 - x_{p_-}$

https://doi.org/10.1017/etds.2020.18 Published online by Cambridge University Press

should be considered negative. More generally, the lattice site and time of the nth collision, $n \geqslant 1$, can be computed from k_j for $j = 0, \ldots, n$ recursively as

$$c_n = c_{n-1} + \left\lfloor \frac{k_n - k_{-n}}{2} \right\rfloor, \quad t_n = t_{n-1} + \mathfrak{a} + \left\lfloor \frac{k_n + k_{-n}}{2} \right\rfloor,$$

which can readily be written as explicit summations. In particular, the collision sites remain constant as long as $k_j = k_{-j}$ for an interval $j \in [j_-, j_+] \subset \mathbb{N}$.

We point out an analogy to so-called coherent structures found in nonlinear waves in partial differential equations, in particular the complex Ginzburg–Landau equation. In all cases we require collision times to be equidistant, that is, $t_{n+1} - t_n = \mathfrak{a} + \tau$, $\tau \in \mathbb{N}$, which means $k_{n+1} + k_{-n-1} = \tau$. We may view x as a *sink defect*, if the collision sites move with constant speed s, that is,

$$\frac{c_{n+1} - c_n}{t_{n+1} - t_n} = s \;\Leftrightarrow\; c_{n+1} = c_n + s(\mathfrak{a} + \tau).$$

However, since there is no dispersion of waves and thus no variation of group velocity, using this terminology is a slight abuse of language.

By manipulating c_n, t_n, we can create a richer set of orbits whose complexity can be measured by the topological entropy discussed later. One may interpret this as the entropy of the admissible sequences of pairs $(c_n, t_n)_{n\in\mathbb{N}} \subset \mathbb{Z} \times \mathbb{N}$, though we do not pursue this viewpoint here.

Rather we use the waiting time coding to investigate the sensitivity of the dynamics. Note that also any $x \in Z$ has 'waiting times', that is, lengths of zero intervals between local pulses forming a sequence $(k_j)_{j\in J}$, where either $J = \mathbb{Z}$ or $J = [-\infty, j_+]$ with $j_+ \geqslant 0$ and $k_{j_+} = \infty$, or $j = [j_-, \infty]$, $j_- \leqslant 0$, $k_{j_-} = \infty$.

Moreover, one can use this coding to argue that the basin of attraction of 0_∞ is dense in X.

COROLLARY 3.10. $\Gamma_-(0_\infty) := \bigcup_{n\in\mathbb{N}} T^{-n}(0_\infty)$ *is dense in* X. *In particular,* $M \cap \Gamma_-(0_\infty)$ *is dense in* $M \in \{Y, Z\}$ *with respect to the subspace topology. Analogously, any* $x \in Z$ *has a dense basin of attraction.*

Proof. It suffices to prove $[a_0, \ldots, a_n]_m \cap \Gamma_-(0_\infty) \neq \varnothing$ for all cylinder sets. To this end, let $x_{[m,m+n]} = (a_0, \ldots, a_n)$. Choose $x_{[-\infty,m-1]} \in S_{\mathrm{R}}^-$ and $x_{[m+n+1,+\infty]} \in S_{\mathrm{L}}^+$ with finitely many waiting times $(k_j)_{j\in J}$ and corresponding pairs (c_n, t_n), respectively, such that there exist counter-propagating local pulses which annihilate pairwise and $x_i = 0$, $|i| \geqslant j$, for sufficiently large $j \in \mathbb{Z}$. Then, $T^{t_N}(x) = 0_\infty$ for some maximal collision time $t_N \in \mathbb{N}$. □

PROPOSITION 3.11. *The subsystem* $(T|_Z, Z)$ *is chaotic in the sense of Devaney: (i) periodic orbits are dense, (ii) it is topologically transitive, and (iii) sensitive with respect to initial conditions. In particular,* Z *is contained in the non-wandering set* $Z \subset \Omega$.

Proof. (i) It is well known that the statements holds for both invariant subsystems S_{R} and S_{L}. Without loss of generality, let $x \in Z \setminus (S_{\mathrm{R}} \cup S_{\mathrm{L}})$ with $x = (x^{\mathrm{R}}, 0_\ell, x^{\mathrm{L}})$, $\ell \in \mathbb{N}$, and $I_{\mathrm{sp}} = [p_-, p_+]$, $x_{[p_-,p_+]} = (1, 0_\ell)$ for suitable $(x^{\mathrm{R}}, x^{\mathrm{L}}) \in S_{\mathrm{L}}^{\mathrm{R}}$. Consider an arbitrary neighbourhood U of x. Due to the structure of Z and the cylinder topology there are

https://doi.org/10.1017/etds.2020.18 Published online by Cambridge University Press

$k_\pm \in \pm\mathbb{N}$ such that the following holds: $I_{\rm sp} \subset [k_- + 1, k_+ - 1]$, $x_{k_\pm} = 0$ and for any $(\tilde{x}^{\rm R}, \tilde{x}^{\rm L}) \in S_{\rm L}^{\rm R}$ we have $\tilde{x} = (\tilde{x}^{\rm R}, x_{[k_-,k_+]}, \tilde{x}^{\rm L}) \in U$ (with positioning so that $\tilde{x}_{k_+} = x_{k_+}$).

In order to make $\tilde{x}$ time periodic we distinguish even and odd ℓ. In case of even ℓ let $p_m := (p_+ - p_- - 1)/2$ and choose $\tilde{x}^{\rm R}$ as the leftward periodic extension of $x_{[k_-,p_m]}$ and $\tilde{x}^{\rm L}$ the rightward periodic extension of $x_{[p_m+1,k_+]}$. The odd case is analogous.

(ii) Let $U, V \subset Z$ be any open non-empty $f := T|_Z$-invariant sets. For an index set $K, k \in K$ and fixed $a_{0_k}, \ldots, a_{m_k} \in \mathcal{A}$, $n_k \in \mathbb{Z}$, let $C_k^Z := [a_{0_k}, \ldots, a_{m_k}]_{n_k} \cap Z$. With this notation, U and V are of the form $U = \bigcup_{i\in I} C_i^Z$ and $V = \bigcup_{j\in J} C_j^Z$. Since U, V are f-invariant, $f^n(C_i^Z) \subseteq U$ and $f^n(C_j^Z) \subseteq V$ for all $i \in I$, $j \in J$ and $n \in \mathbb{N}$. By Corollary 3.10, there exists some $N \in \mathbb{N}$ such that $0_\infty \in f^N(C_i^Z) \cap f^N(C_j^Z) \subseteq U \cap V$. By [**10**, Corollary 1.4.3], f is topologically transitive.

(iii) This already follows by (i) and (ii) (cf. [**21**]) but can also be shown explicitly. To this end, let $x \in Z \setminus (S_{\rm R} \cup S_{\rm L})$ with waiting times $(k_j)_{j\in J}$. Let U be an arbitrary neighbourhood of x and j_0 such that any change of finite k_j with $|j| \geqslant j_0$ gives a point in U. In particular, unless already $k_{j_0} = \infty$ or $k_{-j_0} = \infty$ we choose x' with waiting times $k'_j = k_j$ for $|j| \leqslant j_0$ (and $j \in J$) such that this holds so that $T^m(x') \in S_{\rm R} \cup S_{\rm L}$ for which sensitivity is straightforward. □

3.3. *Stationary dislocations.* We introduce another class of configurations $x \in X$ related to Z, which possesses at least one *dislocation* at some $j \in \mathbb{Z}$, that is, $s(x_j, x_{j+1}) > 1$, so that $x \notin Z$. Consider first $x \in X$ with $x = (x^{\rm R}\ {}^p|x^{\rm L})$, $x^{\rm R} \in S_{\rm R}^-$, $x^{\rm L} \in S_{\rm L}^+$, with one dislocation at p that is then naturally a generalized separating position. An example is the orbit

$$\begin{aligned} x &= (\ldots, 3, 2\ {}^p|0, 1, 2, \ldots), \\ &\ \ \vdots \\ T^{\mathfrak{a}-1}(x) &= (\ldots, a, 0\ {}^p|\mathfrak{a}-1, \mathfrak{a}, 0, \ldots), \\ T^{\mathfrak{a}}(x) &= (\ldots, a'\ {}^p|\mathfrak{a}, 0, b, \ldots), \\ T^{\mathfrak{a}+1}(x) &= (\ldots, a''\ {}^p|0, b', \ldots). \end{aligned}$$

For $a = 0$, we have $a' = 0$ and possibly $a'' = 1$, and, since $b' \in \{0, 1\}$, the next pulse collision would be as in Z. Hence, maintaining a difference from Z requires maintaining a dislocation at the separating position p. The simplest option is $a = b = 1$ so that $a' = 1$ and $a'' = 2$ so that the same dislocation as in x occurs. Let $x^{\rm R*\pm}$ and $x^{\rm L*\pm}$ be the highest-frequency pulse sequence with one 0 between local pulses left-infinite ('$-$') or right-infinite ('$+$'). Choosing $x^{\rm R} = x^{\rm R*-}$, $x^{\rm L} = x^{\rm L*+}$ creates a periodic orbit with period $\mathfrak{a}+1$ and constant separating position. This construction generalizes to any choice of x_p, x_{p+1}, and we refer to such a periodic solution, as well as the following ones, as *periodic stationary dislocation*.

In fact, we may place dislocations next to each other as long as one neighbour at each 0 lies in E. This yields an interval of dislocations of arbitrary width between $x^{\rm R*-}$ and $x^{\rm L*+}$, and the width and position of the dislocations for such a solution remain constant and the solutions has period $\mathfrak{a}+1$; cf. Figure 5(d). Moreover, for $s(x_j, x_{j+1}) \in E$, excitations are

https://doi.org/10.1017/etds.2020.18 Published online by Cambridge University Press

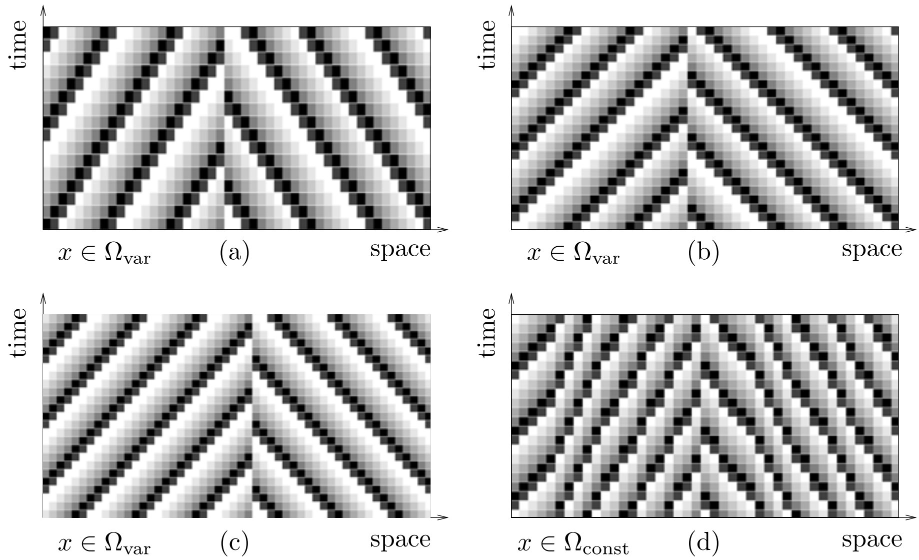

FIGURE 5. Snapshots of configurations with (spatially) stationary dislocations (again $e = 2$ and $r = 4$ with the same grey levels as for Figure 4). Parts (a)–(c) show configurations in Ω_{var} with unique separating position (dislocation). Part (d) illustrates an element of Ω_{const} with an interval of separating positions (dislocations); cf. §4.3.1 and 4.3.2 for details. Note that, in time, the dislocations are either periodic as suggested in (a) and (c) or aperiodic as in (b).

transported from right to left so that we may take an interval of such dislocation between $x^{\mathrm{R}*-}$ and $x^{\mathrm{R}*+}$, thus creating a kind of so-called 'transmission defect'; cf. §3.2.

Notably, if we select to the left x^{R} or to the right x^{L} with a longer waiting times, then the dynamics will map into Z after finitely many steps, except for the following type of stationary dislocations.

For $\mathfrak{a} \geqslant 4$, $r > e + 1$, there is a class of stationary dislocations with arbitrarily long period, even aperiodic, having a unique separating position. Consider the $(x^{\mathrm{L}}, x^{\mathrm{R}}) \in S_{\mathrm{L}}^{\mathrm{R}}$ with pulse distances periodically alternating between one and two (cf. Figure 5(a)):

$$x^{\mathrm{L}} = (0, 0, 1, 2, \ldots, \mathfrak{a}, 0, 1, 2, \ldots, \mathfrak{a}, 0, 0, 1, 2, \ldots, \mathfrak{a}, 0, 1 \ldots),$$
$$x^{\mathrm{R}} = (\ldots, 1, 0, \mathfrak{a}, \mathfrak{a} - 1, \ldots, 1, 0, 0, \mathfrak{a}, \mathfrak{a} - 1, \ldots, 1, 0, \mathfrak{a}, \ldots, e + 1),$$

and set $x := (x^{\mathrm{R}\ p} | x^{\mathrm{L}})$. Following the dynamics of this initial state gives at $j = e + 2r$ that $T^j(x)_{[p,p+1]} = (\mathfrak{a}, r - 2)$ and $T^{j+1}(x)_{[p,p+1]} = (0, r - 1)$. The assumption $r - 1 \in R$ gives $T^{j+2}(x)_{[p,p+1]} = (0, r)$, which is consistent with the zero block in x^{R} and thus we obtain a periodic solution of minimal period $2\mathfrak{a} + 3$. For more generality, see §4.

In this fashion we can map the full 0–1 shift onto such solutions, thus creating another chaotic invariant subset. However, as shown in §4, this has smaller entropy than Z and the non-wandering set is formed by Z together with the configurations of this subsection.

3.4. *Skew-product structure.* In Proposition 3.5 we showed that $h(Z, T|_Z) = 2 \ln \rho_{\mathfrak{a}}$, and that it is combinatorially generated by Z_∞; cf. Remark 3.6. This value is exactly the sum of the topological entropies of the left and right subshifts (cf. Lemma 3.4(i)) for which

https://doi.org/10.1017/etds.2020.18 Published online by Cambridge University Press

$h(S_R, T|_{S_R}) = h(S_L, T|_{S_L}) = \ln \rho_{\mathfrak{a}}$. Thus, the well-known product formula $h(\sigma_L \times \sigma_R) = h(\sigma_L) + h(\sigma_R)$ suggests a product structure of the dynamics of T on Z. Indeed, if, for some $x \in Z$, two pulses approach each other under T, the dynamics is exactly a combination of left and right shifts. However, once two pulses have annihilated, the position of the next annihilation can be arbitrarily far away, which causes problems in finding a conjugacy of T on Z to some form of product system.

Here we present a topological conjugacy to a skew-product system for the restriction to Z_∞. Note that restricting on the dense subset $Z_\infty \subset Z$ makes no difference in terms of the Bowen–Dinaburg entropy.

PROPOSITION 3.12. $h(Z, T|_Z) = h(Z_\infty, T|_{Z_\infty})$

Proof. Since Z is a totally bounded metric space and $Z_\infty \subset Z$ is dense by Lemma 3.4(iv), this is a direct consequence of [**7**, Corollary 4]. □

Consider the left and right subshifts placed at fixed positions,

$$\Sigma_L^+ := \{x = (x_i)_{i \in \mathbb{Z}_{>0}} \in \mathcal{A}^{\mathbb{Z}_{>0}} : a_{x_i, x_{i-1}} = 1\},$$
$$\Sigma_R^- := \{x = (x_i)_{i \in \mathbb{Z}_{\le 0}} \in \mathcal{A}^{\mathbb{Z}_{\le 0}} : a_{x_i, x_{i+1}} = 1\},$$

on which the standard right shift $\sigma_{R,-}$ and left shift $\sigma_{L,+}$ are defined with pseudo-inverses for $m < 0$ given by

$$\sigma_{R,-}^m((\ldots, x_{-1}, x_0)) := (\ldots, x_{-1}, x_0, 0_m), \quad \sigma_{L,+}^m((x_0, x_1, \ldots)) := (0_m, x_0, x_1, \ldots).$$

Each configuration $x \in Z_\infty$ can be written as $x = (x^R\ {}^p|\ x^L)$ with $x^R \in \Sigma_R^- \setminus \{0_\infty^-\}$ and $x^L \in \Sigma_L^+ \setminus \{0_\infty^+\}$. Here $p \in \mathbb{Z}$ is some separating position and hence *a priori* not unique. Since separating positions form an interval $I_{sp}(x) = [p_-, p_+]$, with $p_\pm = p_\pm(x)$, one option for a unique choice is the *middle separating position*

$$p_{mid}(x) := \left\lfloor \frac{p_+(x) + p_-(x)}{2} \right\rfloor.$$

For $x = (x^R\ {}^p|\ x^L) \in Z_\infty$ we define the *adaption of p to the middle separating position of Tx* by $a\colon Z_\infty \to \mathbb{Z}$, $a(x) := p_{mid}(Tx) - p$.

While the adaption in Z_∞ is always bounded there is no *a priori* bound after pulse collisions. As long as p_{mid} is constant during iteration of T, that is, $a(T^i x) = 0$ for an interval in $\mathbb{N}$, the dynamics of T is a product of left and right shifts centred at position $p = p_{mid}(x)$,

$$T(x) = (\sigma_{R,-}(x)\ {}^p \mid \sigma_{L,+}(x)).$$

This occurs in an invariant subset of Ω (cf. proof of Theorem 4.6), but otherwise the description requires some technicalities.

We look for a set $\mathcal{Z}$ and a map $F\colon \mathcal{Z} \to \mathcal{Z}$, which is in essence a product of left and right shifts and admits an appropriate continuous conjugation $H\colon Z_\infty \to \mathcal{Z}$, that is, $H \circ T|_{Z_\infty} = F \circ H$ obeys a commutative diagram

$$\begin{array}{ccc} Z_\infty & \xrightarrow{T} & Z_\infty \\ {\scriptstyle H}\downarrow & & \downarrow{\scriptstyle H} \\ \mathcal{Z} & \xrightarrow{F} & \mathcal{Z} \end{array}$$

To this end, let $\Sigma^+_- := \Sigma^-_{\mathrm{R}} \times \Sigma^+_{\mathrm{L}} \setminus \Sigma_*$, where $(x^{\mathrm{R}}, x^{\mathrm{L}}) \in \Sigma_*$ if $x = (x^{\mathrm{R}\ 0}|\ x^{\mathrm{L}})$ does not lie in Z_∞, which is precisely the case if $x \in S^{\mathrm{R}}_{\mathrm{L}}$ has a dislocation at the block $x_{[0,1]} = (x^{\mathrm{R}}_0, x^{\mathrm{L}}_1)$ or if $x \in S^{\mathrm{R}}_{\mathrm{L}}$ with $x_{[-\infty,k]} = 0^-_\infty$ or $x_{[k',\infty]} = 0^+_\infty$ for some $k, k' \in \mathbb{Z}$.

On the product space $\mathcal{Z} := \Sigma^+_- \times \mathbb{Z}$ define the skew-product map

$$F: \mathcal{Z} \to \mathcal{Z},\ F(z) = (f(x), g_x(p)), \quad z = (x, p) \in \mathcal{Z},$$

with base function $f: \Sigma^+_- \to \Sigma^+_-$,

$$f(x) = (\sigma^{-\alpha+1}_{\mathrm{R},-}(x^{\mathrm{R}}), \sigma^{\alpha+1}_{\mathrm{L},+}(x^{\mathrm{L}})), \quad x = (x^{\mathrm{R}}, x^{\mathrm{L}}) \in \Sigma^+_-,$$

where $\alpha = a(x^{\mathrm{R}\ 0}|\ x^{\mathrm{L}})$, $\sigma^{-\alpha+1}_{\mathrm{R},-} = \sigma^{-\alpha}_{\mathrm{R},-} \circ \sigma_{\mathrm{R},-}$ and $\sigma^{\alpha+1}_{\mathrm{L},+} = \sigma^{\alpha}_{\mathrm{L},+} \circ \sigma_{\mathrm{L},+}$.

For given $x = (x^{\mathrm{R}}, x^{\mathrm{L}}) \in \Sigma^+_-$, the fibre function $g_x : \mathbb{Z} \to \mathbb{Z}$ is defined as

$$g_x(p) = p + a(x^{\mathrm{R}\ 0}|\ x^{\mathrm{L}}).$$

Finally, the bijection $H: Z_\infty \to \mathcal{Z}$ and its inverse H^{-1} are given by

$$H(x) = (x^{\mathrm{R}}, x^{\mathrm{L}}, p_{\mathrm{mid}}(x)), \quad H^{-1}((x^{\mathrm{R}}, x^{\mathrm{L}}, p)) = (x^{\mathrm{R}\ p}|\ x^{\mathrm{L}}).$$

The natural topology on Σ^+_- in this context is given by the product of the cylinder topologies on Σ^-_{R} and Σ^+_{L}, respectively; taking the product topology with the discrete topology on $\mathbb{Z}$ then gives the topology of $\mathcal{Z} = \Sigma^+_- \times \mathbb{Z}$. Each block $x_{[m,n]}$, $m, n \in \mathbb{Z}$, of Z_∞ either is a block in $S_{\mathrm{L}} \cup S_{\mathrm{R}}$ or contains a separating position in $[m, n]$. In the latter case, it follows that the image under H of a cylinder defined by this block gives a product of non-empty cylinders in Σ^-_{R} and Σ^+_{L}. If a cylinder is defined by a block in S_{L} or S_{R} its image under H is a union of cylinders defined by extended blocks with a separating position, and therefore open in $\mathcal{Z}$. Hence, H is continuous, and similarly we infer continuity of H^{-1}.

Though instructive, the conjugacy does not directly help to determine or sharply estimate the topological entropy. Indeed, since Z_∞ is not compact, it would be desirable to identify a conjugacy for $Z = \overline{Z_\infty}$. However, it is unclear how to track positions that separate left and right shifts in a consistent manner; for example, 0_∞, the bi-infinite zero sequence, does not have a canonical separating position. For elements in $S_{\mathrm{R}} \cup S_{\mathrm{L}}$ one may choose $\pm\infty$ as a separating position, but the preimages of elements with a semi-infinite zero sequence are not unique. Attempts to consider quotient spaces cause additional difficulties in determining the topological entropy in the skew-product system.

4. *The non-wandering set and the topological entropy*

We now turn our attention to T on the entire space X. The aim of this section is to determine the non-wandering set which turns out to consist of the collision subsystem Z and the stationary dislocations. This allows us to determine the topological entropy by inferring the upper estimate $h(X, T) \leqslant h(Z, T|_Z)$.

We first recall the definition of the non-wandering set [**10**, **20**].

Definition 4.1. Let $\theta: \Lambda \to \Lambda$ be continuous on a topological space Λ. The set

$$\Omega(\theta) := \{x \in \Lambda : \text{ for every neighbourhood } U \text{ of } x\ \exists N \geqslant 1 : \theta^N U \cap U \neq \varnothing\}$$

is called the non-wandering set of θ. For compact Λ, one can equivalently assume that there exist arbitrarily large $N \in \mathbb{N}$ for which the intersection is non-zero [**10**]. When θ and Λ are clear from the context, we write Ω instead of $\Omega(\theta)$.

https://doi.org/10.1017/etds.2020.18 Published online by Cambridge University Press

Remark 4.2. For the product topology on $X = \mathcal{A}^{\mathbb{Z}}$, a configuration $x \in X$ is non-wandering, that is, $x \in \Omega(T)$, if and only if for any cylinder set $[x_n, \ldots, x_{n'}]_n$ there exist arbitrary large $N \in \mathbb{N}$ such that $T^N([x_n, \ldots, x_{n'}]_n) \cap [x_n, \ldots, x_{n'}]_n \neq \varnothing$.

For our set-up, $\Omega(T)$ is contained in the eventual image $Y := \bigcap_{n\in\mathbb{N}} T^n(X)$. Since we make use of $\Omega(T) \subset Y$, we prove this inclusion here for completeness.

LEMMA 4.3. *Let Λ be a compact Hausdorff space with a continuous transformation $\theta \colon \Lambda \to \Lambda$. Then the non-wandering set is contained in the eventual image, that is, $\Omega(\theta) \subseteq \bigcap_{n\in\mathbb{N}} \theta^n(\Lambda)$.*

Proof. Let $n \in \mathbb{N}$ and $x \in U := \theta^n(\Lambda)^C$. U is an open neighbourhood of x with

$$\theta^m(U) \subseteq \theta^n(\Lambda) = U^C, \quad \text{for all } m \geqslant n.$$

By [**20**, Theorem 5.7], x is a wandering point. Hence $\Omega(\theta) \subseteq \bigcap_{n\in\mathbb{N}} \theta^n(\Lambda)$. □

Remark 4.4. In the degenerate case $e = r = 1$, the non-wandering set and the eventual image coincide, $Z = \Omega = Y$ [**19**].

4.1. *Strategy for characterizing* Ω. The aim of this section is to characterize the non-wandering set. In this regard, Remark 4.2 provides some guidance: an element $x \in X$ is contained in Ω exactly if any finite block $x_{[n,n']}$ of x can be restored infinitely often at the same positions under iterations of T. In particular, this requires the local dynamics of the blocks to be globally synchronized.

Our strategy to reveal this matching of local and global dynamics is as follows.

(I) *Local analysis.* We start with a local analysis of non-wandering points at each position $p \in \mathbb{Z}$ and show that, for $x \in \Omega$, the trajectory $\{(T^m(x))_{[p,p+1]} : m \in \mathbb{N}_0\}$ of a 2-block $x_{[p,p+1]}$ can be completely described in terms of the transitions of the associated step size

$$s_p^m(x) := s((T^m(x))_p, (T^m(x))_{p+1}) = (T^m(x))_{p+1} - (T^m(x))_p \mod (\mathfrak{a}+1),$$

which decompose into equivalence classes ('communicating classes'); cf. Figures 7 and 8.

(II) *Global analysis.* We use the local step-size analysis to infer the spatial structure of $x \in \Omega$ by showing that the local dynamics of any 2-block $x_{[p,p+1]}$ essentially determines the global spatial structure.

By this approach, we characterize Ω and the topological entropy $h(\Omega, T|_\Omega)$. More specifically, we will identify sets Ω_{const} and Ω_{var} that correspond to (periodic or aperiodic) configurations with stationary dislocations of certain constant or varying step sizes. These form the complement of Z within Ω and the main results of this section are as follows.

THEOREM 4.5. *The non-wandering set, Ω, of the one-dimensional (1D) Greenberg–Hastings cellular automaton associated with $T : X \to X$ can be decomposed into the invariant sets*

$$\Omega = Z \uplus \Omega_{\text{const}} \uplus \Omega_{\text{var}},$$

where $\Omega_{\text{var}} = \varnothing$ if and only if $r \leqslant e + 1$.

https://doi.org/10.1017/etds.2020.18 Published online by Cambridge University Press

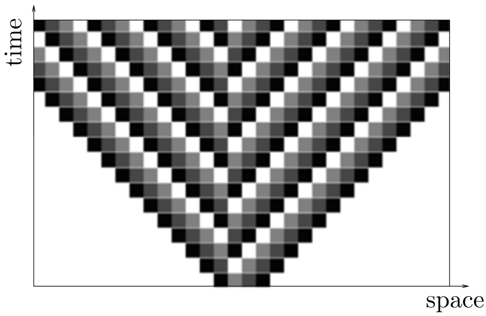

FIGURE 6. One-dimensional spiral: $e = 2$, $r = 1$ (0 shown in white; 1, 2, 3 in lightening grey levels).

The proof will be given in §4.3.

THEOREM 4.6. *The topological entropy, $h(X, T)$, of the 1D Greenberg–Hastings cellular automaton with $e, r \in \mathbb{N}$ is given by $h(X, T) = h(Z, T|_Z) = 2 \ln \rho_{\mathfrak{a}}$, where $\rho_{\mathfrak{a}}$ is the positive root of $x^{\mathfrak{a}+1} - x^{\mathfrak{a}} - 1$. Moreover, $h(\Omega_{\text{const}}, T|_{\Omega_{\text{const}}}) = 0$ and $0 < h(\Omega_{\text{var}}, T|_{\Omega_{\text{var}}}) < 2 \ln \rho_{\mathfrak{a}}$ for $r > e + 1$.*

The proof will be given in §4.4.

Remark 4.7. These results imply that the recurrent structure for $r \leqslant e + 1$ is somewhat simpler since $\Omega_{\text{var}} = \varnothing$. However, somewhat surprisingly in this situation, new wave phenomena occur in the eventual image: an interesting case are sources emitting pulses to the left and right antisynchronously; cf. Figure 6. These qualitatively share features of *1D spirals* observed experimentally in a quasi-1D chemical system and, in continuous models, were related to localized periodic Turing states [**16**]. Here the asymptotic state is $(\mathfrak{a} + 1)$-periodic and lies in Ω_{const}.

In what follows, the step sizes $s_p^m(\cdot)$, as elements of the communicating classes, should not be confused with the states of the cellular automata since both are contained in $\mathcal{A}$ but obey different transition rules.

4.2. *Local analysis.* In this section we analyse the dynamics of 2-blocks $x^m_{[p,p+1]} = (x^m_p, x^m_{p+1})$ under iterations of T. Here, x^m_k is shorthand for $(T^m(x))_k$ with $k \in \mathbb{Z}$ and $m \in \mathbb{N}_0$. Each such 2-block has an associated step size $s^m_p(x) = s(x^m_p, x^m_{p+1}) \in \mathcal{A}$. For space–time windows $[p, p'] \times [m, m']$ of x and s we write, for example, $x^{[m,m']}_{[p,p']}$.

The following lemma is fundamental to our approach.

LEMMA 4.8. *The step size of a 2-block $x_{[p,p+1]}$ for some $p \in \mathbb{Z}$ changes under T at time m, that is, $s^m_p(x) \neq s^{m+1}_p(x)$, if and only if either $(x^m_p, x^{m+1}_p)^\intercal = (0, 0)^\intercal$ or $(x^m_{p+1}, x^{m+1}_{p+1})^\intercal = (0, 0)^\intercal$.*

Specifically, the step size changes if and only if either

$$\text{(i)}\quad x_{[p,p+1]}^{[m,m+1]} = \begin{pmatrix} 0 & c+1 \\ 0 & c \end{pmatrix}, \quad c \in R \cup \{0\}, \textit{ or}$$

$$\text{(ii)}\quad x_{[p,p+1]}^{[m,m+1]} = \begin{pmatrix} c+1 & 0 \\ c & 0 \end{pmatrix}, \quad c \in R \cup \{0\}.$$

Moreover, the step-size change is either
(i) *an increment and* $s_p^{[m,m+1]}(x) = (c, c+1)^\intercal$*, or*
(ii) *a decrement and* $s_p^{[m,m+1]}(x) = (-c, -c-1)^\intercal$ *with* $-c \in \{0, 1, \ldots, r\} \Leftrightarrow c \in R \cup \{0\}$.

Proof. Let us first suppose that $(x_p^m, x_p^{m+1})^\intercal = (0, 0)^\intercal$ and $(x_{p+1}^m, x_{p+1}^{m+1})^\intercal \neq (0, 0)^\intercal$. Three further cases have to be distinguished.
(1) $x_{p+1}^m \neq 0$ and $x_{p+1}^{m+1} \neq 0$. Then, $x_{p+1}^m = c \in \mathcal{A} \setminus \{0, \mathfrak{a}\}$ and, consequently, $x_{p+1}^{m+1} = c+1 \in \mathcal{A} \setminus \{0, 1\}$.
(2) $x_{p+1}^m = 0$ and $x_{p+1}^{m+1} \neq 0$. In this case, we have $x_{p+1}^{m+1} = 1$.
(3) $x_{p+1}^m \neq 0$ and $x_{p+1}^{m+1} = 0$. This implies $x_{p+1}^m = \mathfrak{a}$.
In all three cases, the step size increases and, by symmetry, the step size decreases if $(x_p^m, x_p^{m+1})^\intercal \neq (0, 0)^\intercal$ and $(x_{p+1}^m, x_{p+1}^{m+1})^\intercal = (0, 0)^\intercal$.

For the other direction, suppose

$$s_p^m(x) = x_{p+1}^m - x_p^m \neq x_{p+1}^{m+1} - x_p^{m+1} = s_p^{m+1}(x). \tag{14}$$

For a proof by contradiction, we consider the following two cases.
(4) $(x_p^m, x_p^{m+1})^\intercal = (0, 0)^\intercal = (x_{p+1}^m, x_{p+1}^{m+1})^\intercal$.
(5) $(x_p^m, x_p^{m+1})^\intercal \neq (0, 0)^\intercal \neq (x_{p+1}^m, x_{p+1}^{m+1})^\intercal$.
In the first case, condition (14) does obviously not hold. In the second case, a case-by-case analysis of all possibilities shows that

$$((x_p^m, x_p^{m+1})^\intercal, (x_{p+1}^m, x_{p+1}^{m+1})^\intercal) \in \{(0, 1)^\intercal, (\mathfrak{a}, 0)^\intercal, (a, a+1)^\intercal : a \in \mathcal{A} \setminus \{0, \mathfrak{a}\}\}^2.$$

For each such element, it is easy to verify that the step size remains constant, that is, $s_p^m(x) = s_p^{m+1}(x)$, contradicting condition (14). □

Lemma 4.8 precisely describes how step sizes can and cannot change. In order to make the implications transparent, we introduce the concept of communicating classes. For an arbitrary configuration $x \in X$, position $p \in \mathbb{Z}$ and time $m \in \mathbb{N}_0$, we first define the graph of all possible step-size transitions $s_p^m(x) \mapsto s_p^{m+1}(x)$.

Definition 4.9. We denote by $\mathcal{G}_s$ the directed graph of local step-size transitions: the set of nodes of $\mathcal{G}_s$ is $\mathcal{A}$, and $\mathcal{G}_s$ possesses an edge from s_1 to s_2 for $s_1, s_2 \in \mathcal{A}$ if there exist a configuration $x \in X$, a position $p \in \mathbb{Z}$ and a time $m \in \mathbb{N}$ such that $s_p^{[m,m+1]} = (s_1, s_2)^\intercal$. In this case we say there exists a transition from s_1 to s_2 in $\mathcal{G}_s$ for which we use the notation $s_1 \to s_2$; if $s_1 = s_2$, a transition is called trivial, otherwise non-trivial.

Definition 4.10. Let $s_1, s_2 \in \mathcal{A}$ and τ be the transition $s_1 \to s_2$. $i(\tau) = s_1$ and $t(\tau) = s_2$ are called the *initial* and *terminal state* of τ, respectively. A path P on $\mathcal{G}_s$ is a finite sequence

$P = (\tau_i)_{1 \leqslant i \leqslant m}$ of transitions τ_i such that $t(\tau_i) = i(\tau_{i+1})$ for $1 \leqslant i \leqslant m - 1$. We say that s_1 *communicates* with s_2, if there exist paths from s_1 to s_2 and vice versa, that is, paths $P = (\tau_i)_{1 \leqslant i \leqslant m}$ and $P' = (\tau'_i)_{1 \leqslant i \leqslant m'}$ with $i(\tau_1) = s_1$, $t(\tau_m) = s_2$ and $i(\tau'_1) = s_2$, $t(\tau'_{m'}) = s_1$.

As defined in Definition 4.9, *communication* is an equivalence relation, hence $\mathcal{A}$ is partitioned into equivalence classes, referred to as *communicating classes*, with respect to the step-size transitions. The graph $\mathcal{G}_s$ contains irreducible subgraphs associated with these classes; cf. [**12**]. In particular, the induced graph $\mathcal{G}_C$ whose directed edges stem from connections between the communicating classes has *no loops*. Before deriving the edge set and the structure of these equivalence classes, we remark on the implications for the non-wandering set.

Remark 4.11. Since any 2-block $x_{[p,p+1]}$ of a non-wandering point $x \in \Omega$ must reappear under the dynamics of T, so does the step size $s_1 = s_p(x)$. Hence, if the step size changes to a value s_2, which does not communicate with s_1, then $x \notin \Omega$. In other words, if $x \in \Omega$ and $p \in \mathbb{Z}$, the step sizes $s_p^m(x)$ for any $m \in \mathbb{N}$ lie in the same communicating class.

LEMMA 4.12. *Let $s_1, s_2 \in \mathcal{A}$. Then $\mathcal{G}_s$ has an edge from s_1 to s_2 if and only if either*

(i) $s_2 = s_1 + 1$ *and* $s_1 \in \{0, e+1, \ldots, \mathfrak{a}\} = R \cup \{0\}$, *or*

(ii) $s_2 = s_1 - 1$ *and* $s_1 \in \{0, 1, \ldots, r\}$, *or*

(iii) $s_2 = s_1$.

Specifically, $s_1 \to s_2$ if and only if either $s_1 = s_2$ or $|s_2 - s_1| = 1$ and $s_1, s_2 \in C_0 \cup C_\pi$, where $C_0 := \{\mathfrak{a}, 0, 1\}$ and $C_\pi := \{e+1, \ldots, r\}$ if $r \geqslant e+1$, while $C_\pi = \varnothing$ otherwise. In particular, the communicating classes of $\mathcal{G}_s$ are

$$C_0,\ C_\pi,\ C_a := \{a\},\ a \in \mathcal{A} \setminus (C_0 \cup C_\pi).$$

Proof. Cases (i) and (ii) are a direct consequence of Lemma 4.8. Case (iii) follows from $s_p^m(x) = s_p^{m+1}(x)$ if $x_p^m = x_{p+1}^m > 0$ and the possibility that $x_p^{m+1} = x_{p+1}^{m+1} = 0$ if $x_p^m = x_{p+1}^m = 0$.

Case (iii) means trivial transitions always occur, and it follows that a non-trivial transition is present precisely when cases (i) and (ii) occur jointly (i.e., the intervals overlap; cf. Figure 9). This in turn implies the communicating classes; cf. Figure 7. □

Remark 4.13. It follows that for $x \in \Omega$ with $s_p(x) \in C_a$, $a \notin \{0, \pi\}$, the step size at p remains constant. Step-size transitions are possible within C_0 and, if $r > e+1$, within C_π only. Note that for $e + 1 = r$ we have $C_\pi = \{e+1\}$ so that the step size cannot change in this class.

Remark 4.14. If $s_{p,m}(x) \in C_\pi$ then for c in Lemma 4.8 we have $c \in C_\mathfrak{a} \setminus \{r\}$ since otherwise $s_p^{m+1}(x) = r + 1 \in C_{r+1}$; analogously, $c \neq e+1$. Therefore, whenever $x_p^m = 0$ (respectively, $x_{p+1}^m = 0$), the neighbour state x_{p+1}^m (respectively, x_p^m) is a refractory state, which implies that the dynamics on the space–time windows $[-\infty, p] \times \mathbb{N}$ and $[p+1, +\infty] \times \mathbb{N}$ are independent of each other.

Let us describe the non-trivial transitions in more detail; for generality, we consider configurations $x \in \mathcal{A}^\mathbb{K}$, $\mathbb{K} \in \{\mathbb{Z}, \mathbb{Z}_{\leqslant q}, \mathbb{Z}_{\geqslant q} : q \in \mathbb{Z}\}$.

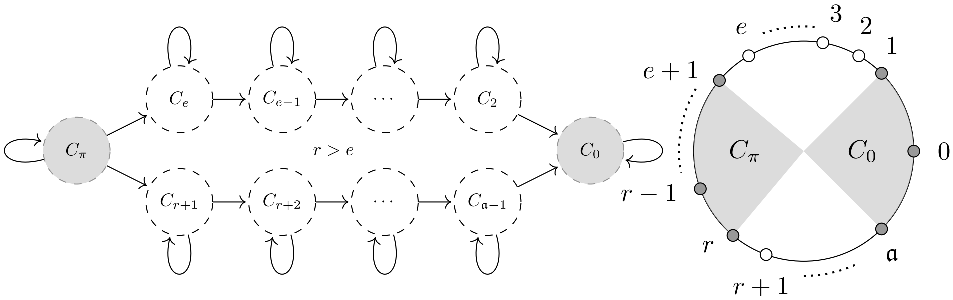

FIGURE 7. Macrostructure of the communicating classes. Transition graph $\mathcal{G}_C$ of the step-size dynamics of 2-blocks for $r > e$ (left) with vertex set consisting of the communicating classes which contain either one single state or multiple states as illustrated on the unit circle (right). In particular, $C_\pi = \{e+1\}$ for $r = e+1$ and $\#C_\pi > 1$ for $r > e+1$.

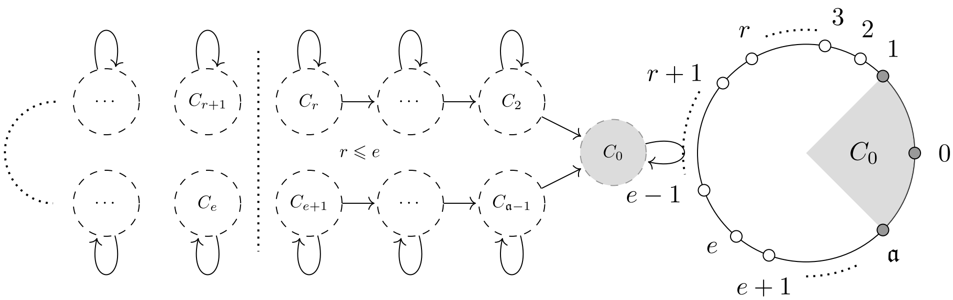

FIGURE 8. Transition graph $\mathcal{G}_C$ for $r \leqslant e$. In this case $C_\pi = \varnothing$.

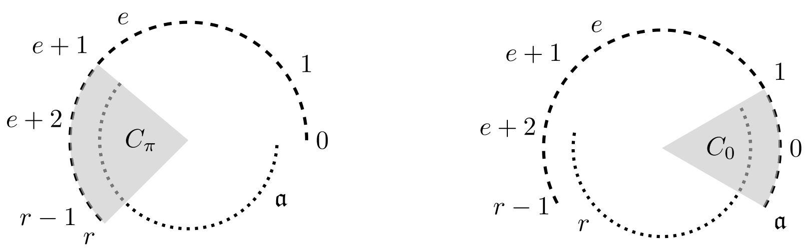

FIGURE 9. The inner dotted arcs represent step sizes $s_1 \in R \cup \{0\}$ (left) and their increments $s_2 = s_1 + 1$ (right). The outer dashed arcs show the step sizes $s_1 \in \{0, 1, \ldots, r\}$ (left) and their decrements $s_2 = s_1 - 1$ (right). The maximal overlapping is given by $C_0 \cup C_\pi$ (shadowed region).

Definition 4.15. Let $x \in \mathcal{A}^{\mathbb{K}}$, p, $p+1 \in \mathbb{K}$ and $j \in \{0, \pi\}$. If $j = \pi$, assume $r > e+1$. For some interval $\mathcal{I} \subseteq \mathbb{N}$, the *transition times at p in C_j* constitute the sequence $(m_i)_{i \in \mathcal{I}}$ of positive integers with $m_i < m_{i+1}$ such that

$$s_p^{m_i}(x) \in C_j \quad \text{and} \quad s_p^{m_i}(x) \neq s_p^{m_i - 1}(x) \quad \text{for all } i \in \mathcal{I}.$$

The transition time m_i is called consecutive if $m_{i+1} = m_i + 1$ or $m_{i-1} = m_i + 1$ and separated otherwise. Times $m > 0$ such that $s_p^m(x) = s_p^0(x)$ are called step returns.

https://doi.org/10.1017/etds.2020.18 Published online by Cambridge University Press

Remark 4.16. Let r_k be a step return time of some $x \in \mathcal{A}^{\mathbb{K}}$. Since step-size changes are by ± 1, for the transition times $m_i \leqslant r$ we have

$$\#\{m_i \leqslant r_k : s_p^{m_i}(x) = s_p^{m_{i-1}}(x) + 1\} = \#\{m_i \leqslant r_k : s_p^{m_i}(x) = s_p^{m_{i-1}}(x) - 1\}. \tag{15}$$

Due to Remarks 4.11 and 4.2, for $x \in \Omega$ the sequence of step returns is infinite.

COROLLARY 4.17. *For $x \in \mathcal{A}^{\mathbb{K}}$, each separated transition time m_i lies in a triple*

$$(x_p^{m_i-1}, x_p^{m_i}, x_p^{m_i+1})^\intercal \in \{(0, 0, 0)^\intercal, (0, 0, 1)^\intercal\} \quad \textit{or}$$
$$(x_{p+1}^{m_i-1}, x_{p+1}^{m_i}, x_{p+1}^{m_i+1})^\intercal \in \{(0, 0, 0)^\intercal, (0, 0, 1)^\intercal\},$$

depending on whether m_i is associated with a step size in C_0 or, if $r > e + 1$, in C_π. If $r > e + 1$, there can be at most $\max\{2, \#C_\pi - 1\}$ *consecutive transition times $m_i < m_{i+1} < \ldots < m_j$. More specifically, if the step sizes associated to the m_k, $i \leqslant k \leqslant j$, are in C_π, the m_k lie in a block*

$$(x_p^{m_i-1}, \ldots, x_p^{m_j+1})^\intercal = (0_\ell, 1)^\intercal \quad \textit{or} \quad (x_{p+1}^{m_i-1}, \ldots, x_{p+1}^{m_j+1})^\intercal = (0_\ell, 1)^\intercal, \tag{16}$$

with a zero block 0_ℓ of length $3 \leqslant \ell \leqslant \#C_\pi$ while there can be exactly two consecutive transition times m_1, m_2 with associated step sizes in C_0 which lie in a quadruple of type (16) or a triple

$$(x_p^{m_1-1}, x_p^{m_1}, x_p^{m_2})^\intercal = (0, 0, 1)^\intercal \quad \textit{or} \quad (x_{p+1}^{m_1-1}, x_{p+1}^{m_1}, x_{p+1}^{m_2})^\intercal = (0, 0, 1)^\intercal.$$

Proof. This is a direct consequence of Lemma 4.12, noting that consecutive transitions increase the length of the zero block in time so that c is incremented further, but these increments cannot be in E before a transition. □

We end this subsection with examples for the macro- and microstructure of the communicating classes when $r > e + 1$ and $e > r$. In the next section we use this local framework of the step-size dynamics to determine the global spatial structure of non-wandering points.

Example 4.18. Let $e = 3$ and $r = 7$. The communicating classes are given by $C_0 = \{0, 1, 10\}$, $C_2 = \{2\}$, $C_3 = \{3\}$, $C_\pi = \{4, 5, 6, 7\}$, $C_8 = \{8\}$ and $C_9 = \{9\}$; see Figure 10.

Example 4.19. Let $e = 7$ and $r = 4$. The communicating classes are given by $C_0 = \{0, 1, 11\}$, $C_2 = \{2\}$, $C_3 = \{3\}$, $C_4 = \{4\}$, $C_5 = \{5\}$, $C_6 = \{6\}$, $C_7 = \{7\}$, $C_8 = \{8\}$, $C_9 = \{9\}$ and $C_{10} = \{10\}$; see Figure 11.

4.3. *Global analysis: characterizing the non-wandering set.* The local analysis showed that, for $x \in \Omega$ and any $p \in \mathbb{Z}$, the step sizes $s_p^m(x)$ for all $m \in \mathbb{N}$ lie in the same communicating class. We also know that all k-blocks $x_{[p,p+k]}$, $k \in \mathbb{N}$, need to reappear infinitely often under T. In this section we infer from this the spatial structure of $x \in \Omega$. Specifically, we show that the class C_0 can be identified with the pulse-collision subsystem Z of §3, and C_π with the non-trivial dislocations of §3.3. To this end, we need the following easy but helpful observation. In what follows, x^{-j} denotes an arbitrary element of $T^{-j}(\{x\})$, if it exists, and x_n^{-j} its nth coordinate.

https://doi.org/10.1017/etds.2020.18 Published online by Cambridge University Press

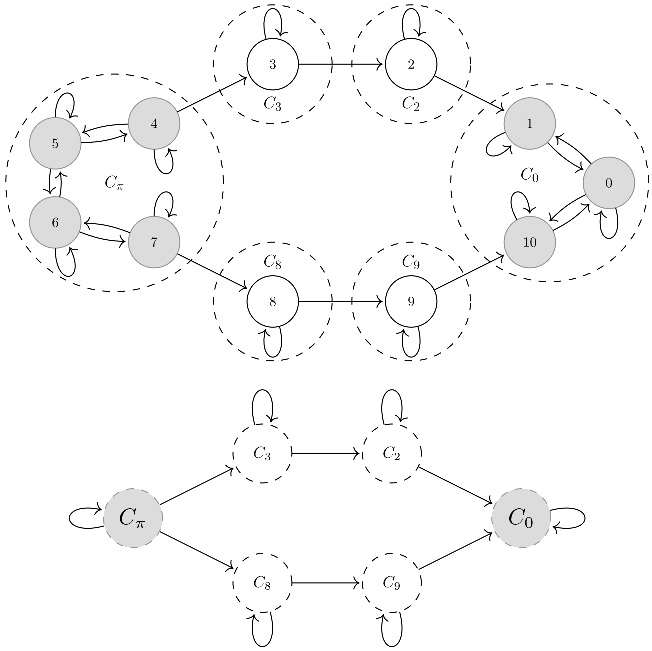

FIGURE 10. Example 4.18. The transition graph $\mathcal{G}_s$ with vertex set $\mathcal{A}$ (top) reveals the microstructure of the communicating classes of the step-size transitions, while the graph $\mathcal{G}_C$ (bottom) illustrates the macrostructure by using the set of communicating classes as the vertex set (cf. Figure 7). For visibility the dashed circles representing C_0 and $C\pi$ are not filled in grey in the top diagram.

LEMMA 4.20. *For $a - 1 \in E \cup R$ and $k \in \mathbb{Z}$, consider $x \in X$ with either $x_{[k,k+1]} = (0, a)$ or $x_{[k-1,k]} = (a, 0)$. If $x_k^{1-a} = c$ exists, then:*

(i) $c = \mathfrak{a} - a + 2$ *if* $a - 1 \in E$;

(ii) $c \in [\mathfrak{a} - a + 2, r + 1]$ *if* $a - 1 \in R$.

Proof. In case (i) we have $x_k^{-1} = \mathfrak{a}$ by the local preimage formula (2), p. 1400, and at least the $\mathfrak{a}$ further local preimages at k are unique and simply decremental: $x_k^{-j} = \mathfrak{a} + 1 - j$, for $1 \leqslant j \leqslant \mathfrak{a} + 1$. Hence, at $j = a - 1$ we have $x_k^{-j} = \mathfrak{a} - a + 2$.

In case (ii) the preimage x_k^{-1} might be $\mathfrak{a}$ or 0. In the first case the same applies as in (i), which gives the lower bound $c = \mathfrak{a} - a + 2$. The same applies to further preimages x_k^{-j}, $j > 1$ until $j = a - e - 1$, for which $x_{k\pm1}^{-j} = e + 1$ (with sign depending on the 2-block). Then the choice $x_{k\pm1}^{-j} = 0$ enforces $x_{k\pm1}^{-j-1} = e + r$ so that $c = \mathfrak{a} - a + 2 = r + 1$, which is the upper bound (note $a > e + 1$ in the present case). □

Now we are in a position to state a characterization of the non-wandering points with step sizes in C_0 only.

LEMMA 4.21. *$x \in \Omega$ and $s_p(x) \in C_0$ for all $p \in \mathbb{Z}$ if and only if $x \in Z$.*

Proof. By definition of Z, it follows that $s_p(x) \in C_0$ for all $p \in \mathbb{Z}$, and we showed $Z \subset \Omega$ in Proposition 3.11.

https://doi.org/10.1017/etds.2020.18 Published online by Cambridge University Press

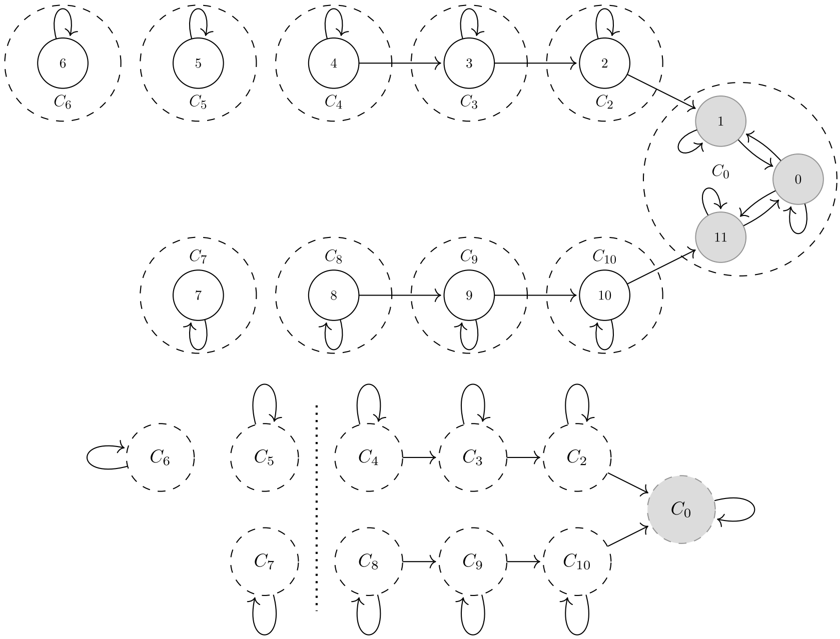

FIGURE 11. Example 4.19. $\mathcal{G}_s$ (top) and $\mathcal{G}_C$ (bottom), cf. Figure 8.

For the converse suppose $x \in \Omega$ and $s_p(x) \in C_0$ for all $p \in \mathbb{Z}$. We will show by contraposition that $x \in Z$. From the definition of Z we immediately infer that the only blocks which might *a priori* occur in x but not in elements of Z are

$$\begin{aligned} F_{3,1} &:= \{(a, a, a) : a \in E \cup R\}, \\ F_{3,2} &:= \{(a, a, b), (b, a, a) : a \in E \cup R, b \in \mathcal{A}, s(a, b) = \mathfrak{a}\}, \\ F_{3,3} &:= \{(a, b, c) \in \mathcal{A}^3 : s(b, a) = \mathfrak{a} \text{ and } s(b, c) = \mathfrak{a}\}, \\ F_n &:= (\mathfrak{a}, 0_{n-2}, \mathfrak{a}), n \geqslant 4. \end{aligned}$$

The idea is to show that blocks contained in these sets (or, more generally, in supersets which are defined below) cannot occur in configurations in the eventual image Y, and hence not in elements of the non-wandering set Ω; cf. Lemma 4.3. This strategy is motivated by our approach to characterize Y as a shift space $X_{\mathcal{F}}$ with respect to forbidden blocks $\mathcal{F}$ which will be the subject of a forthcoming paper.

First, as a direct consequence of the local preimage formula (2), 3-blocks in

$$\mathcal{F}_{3,0} := (\mathcal{A} \setminus (E + 1)) \times \{1\} \times (\mathcal{A} \setminus (E + 1))$$

do not occur in elements of Y.

Regarding $F_{3,1}$, suppose $x \in X$ with $x_{[k,k+2]} = (a, a, a)$ for some $k \in \mathbb{Z}$ and $a \in E \cup R$. Then $x^{-(a-1)}_{[k,k+2]} = (1, 1, 1)$, which lies in $\mathcal{F}_{3,0}$ so that (a, a, a) cannot occur in the eventual image.

Turning to $F_{3,2}$, we show that blocks contained in

$$\mathcal{F}_{3,2} := \{(a, a, b), (b, a, a) : a \in E \cup R, b \in \mathcal{A}, s(a, b) > e\},$$

https://doi.org/10.1017/etds.2020.18 Published online by Cambridge University Press

which is a superset of $F_{3,2}$, do not occur in elements of Y; by symmetry, it suffices to consider the case (a, a, b).

Suppose $x \in X$ with $x_{[k,k+2]} = (a, a, b)$ for some $k \in \mathbb{Z}$ with $a \in E \cup R$, $b \in \mathcal{A}$ and $s(a, b) > e$. We claim that for any choice of preimages we have $x^{1-a}_{[k,k+2]} = (1, 1, c)$ with $c \in \mathcal{A} \setminus (E + 1)$, which lies in $\mathcal{F}_{3,0}$ so that (a, a, b) cannot occur in the eventual image.

For $a < b$, the first $a - 1$ preimages are unique so $x^{1-a}_{[k,k+2]} = (1, 1, b - a + 1)$. Since $b - a + 1 > e + 1$ by assumption, this block lies in $\mathcal{F}_{3,0}$.

If $a > b$ the first $b - 1$ preimages are unique, and assuming that the bth preimage exists (i.e., the right neighbour lies in $E + 1$) gives $x^{-b}_{[k,k+2]} = (a - b, a - b, 0)$ with $a - b \in [2, r]$ (which requires $r > 1$). Lemma 4.20 implies $x^{1-a}_{[k,k+2]} = (1, 1, c)$ with $c \in [\mathfrak{a} - (a - b), r + 2]$ so that $c \in [e + 2, r + 1]$. But then $x^{1-a}_{[k,k+2]}$ lies in $\mathcal{F}_{3,0}$.

Considering $F_{3,3}$, we show that blocks contained in

$$\mathcal{F}_{3,3} := \{(a, b, c) \in \mathcal{A}^3 : s(b, a) > e \text{ and } s(b, c) > e\},$$

which is a superset of $F_{3,3}$, do not occur in Y. For $(a, b, c) \in \mathcal{F}_{3,3}$ and $x \in X$ with $x_{[k,k+2]} = (a, b, c)$ for some $k \in \mathbb{Z}$ we distinguish the following three cases.

(1) For $b \in R$, the assumption $s(b, a), s(b, c) > e$ means $a, c \in [b - r, b - 1]$, and, without loss of generality, by spatial reflection, $a \leqslant c$. Then $x^{-a}_{[k,k+2]} = (0, b - a, c - a)$ with $b - a \in [1, r]$ and $e < s(b, c) = c - b < c - a$ so $c - a \notin E + 1$. Hence, if $b - a = 1$ then $(0, b - a, c - a) \in \mathcal{F}_{3,0}$ so we may assume $b - a \in [2, r]$. It then follows from Lemma 4.20 that $x^{1-b}_{[k,k+2]} = (a', 1, c')$ with $a', c' \geqslant \mathfrak{a} + 2 - (b - a) \geqslant e + 2$ and thus $(a', 1, c') \in \mathcal{F}_{3,0}$.

(2) For $b \in E$, the assumption $s(b, a), s(b, c) > e$ means $a, c \in [0, b - 1] \cup [b + e + 1, \mathfrak{a}]$. The subcase $a, c \in [0, b - 1]$ (take $a \leqslant c$ without loss of generality) yields $x^{-a}_{[k,k+2]} = (0, b - a, c - a)$ with $b - a \in [1, e] \subset [1, r]$ so that case 1 can be applied. If $c \in [b + e + 1, \mathfrak{a}]$ we obtain $c' = c - b + 1 > e + 1$ with c' derived in case 1, and thus also $(a', 1, c') \in \mathcal{F}_{3,0}$. The last subcase $a, c \in [b + e + 1, \mathfrak{a}]$ means $x^{1-b}_{[k,k+2]} = (a - b + 1, 1, c - b + 1) \in \mathcal{F}_{3,0}$ as in the previous subcase.

(3) Finally, assume $b = 0$, which implies $a, c \in R$ (again take $a \leqslant c$ without loss of generality). By Lemma 4.20 we have $x^{1-a}_{[k,k+2]} = (1, b', c - a + 1) =: (a', b', c')$ with $b' \in [\mathfrak{a} + 2 - a, r + 1] \subset [2, r + 1]$ and $c' \in [1, \mathfrak{a} + 1 - a] \subset [1, r + 1]$. Thus $a' - b' \in [-r, a - \mathfrak{a} + 1] \subset [-r, -1]$ and $c' - b' \in [-r, -1]$, and therefore $s(b', a') = \mathfrak{a} + 1 + a' - b' > e$, and $s(b', c') = \mathfrak{a} + 1 + c' - b' > e$.

Turning to F_n, we show by induction that n-blocks, $n \geqslant 4$, of the form $(a, 0, \ldots, 0, b)$ in the superset $\mathcal{F}_n := R \times \{0\}^{n-2} \times R \supset F_n$ do not occur in elements of Y. We consider $n = 4$ first and let $x \in X$ with $x_{[k,k+3]} = (a, 0, 0, b) \in \mathcal{F}_4$ for some $k \in \mathbb{Z}$, where without loss of generality $a \leqslant b$. In case $a = b = e + 1$ we have $x^{-1}_{[k,k+2]} = (e, \mathfrak{a}, \mathfrak{a}) \in \mathcal{F}_{3,2}$. If $a = e + 1$ and $r > e + 1$ we have either $x^{-1}_{[k+1,k+3]} = (\mathfrak{a}, 0, b - 1) \in \mathcal{F}_{3,3}$ or $x^{-1}_{[k+1,k+3]} = (\mathfrak{a}, \mathfrak{a}, b - 1) \in \mathcal{F}_{3,2}$. If $b \geqslant a > e + 1$, we have

$$x^{-1}_{[k,k+3]} \in \{(a - 1, c, d, b - 1) : c, d \in \{0, \mathfrak{a}\}\}$$

and for $c \neq 0$ or $d \neq 0$ we get 3-blocks in $\mathcal{F}_{3,2} \cup \mathcal{F}_{3,3}$, while for $c = d = 0$ the 4-block is contained in $\mathcal{F}_4$. Hence, as long as $x^{-j}_k > e + 1$, the preimage contains a block with non-empty preimage. Eventually, $x^{-j}_k = e + 1$ and we are in one of the previous cases.

https://doi.org/10.1017/etds.2020.18 Published online by Cambridge University Press

Suppose now the statement holds for some $n \geqslant 4$ and let $x \in X$ with $x_{[k,k+n]} = (a, 0_{n-1}, b) \in \mathcal{F}_{n+1}$ for some $k \in \mathbb{Z}$ and, without loss of generality, $a \leqslant b$. If $a = e + 1$, we have either $x^{-1}_{[k,k+2]} \in \mathcal{F}_{3,2}$, $x^{-1}_{[k+1,k+3]} \in \mathcal{F}_{3,3}$ or $x^{-1}_{[k+1,k+n]} \in \mathcal{F}_n$. If $a > e + 1$ we have either one of the previous blocks or $x^{-1}_{[k,k+n]} = (a - 1, 0_{n-1}, b - 1) \in \mathcal{F}_{n+1}$, and this repeats until we end up with $x^{-j}_k = a - j = e + 1$, which is the previous case. □

We next identify trivial, $(\mathfrak{a} + 1)$-periodic dislocations. First, however, we make a simple, but fundamental observation.

LEMMA 4.22. *If $x \in \Omega$ and $s^m_p(x)$ is not constant in $m \in \mathbb{N}$ for some p, then $s^0_q(x) \in C_0 \cup C_\pi$ for all $q \in \mathbb{Z}$ and there is $m \in \mathbb{N}$ such that $x^{[m,m+1]}_p = (0, 0)^\intercal$.*

Proof. The block $x^m_{[p-1,p+1]}$ repeats infinitely many times for $m \in \mathbb{N}$ and any step-size change of $s^m_p(x)$ is compensated by a reverse step; cf. Remark 4.16. Hence, there is $m \in \mathbb{N}$ such that $x^{[m,m+1]}_p = (0, 0)^\intercal$. If $x^m_{p-1} = 0$ we immediately have $s^0_{p-1}(x) \in C_0$. If $x^m_{p-1} \neq 0$ then $s^m_{p-1}(x) \neq s^{m+1}_{p-1}$ and by Lemma 4.12 it follows that $s^0_{p-1} \in C_0 \cup C_\pi$, which are the only classes that allow for changing step sizes. The claim follows by induction on the position. □

The following lemma shows how 'excitations' can be backtracked in time by a spatial shift in one direction, if all step sizes lie in $C_0 \cup C_\pi$. By the previous lemma this is the case if the step size is not constant.

LEMMA 4.23. *Suppose $x \in \Omega$, $s^0_p(x) \in C_0 \cup C_\pi$ for all $p \in \mathbb{Z}$. If there are $m \in \mathbb{N}$, $p \in \mathbb{Z}$ such that $x^m_{p,p+1} = (1, 0)$ then for all $1 \leqslant j \leqslant m$ we have that $x^{m-j}_{p-j,p+1-j} = (1, 0)$. Likewise, $x^m_{p,p+1} = (0, 1)$ implies $x^{m'-j}_{p+j,p+1+j} = (0, 1)$ for all $1 \leqslant j \leqslant m$.*

Proof. By assumption, $x^{[m-1,m]}_{[p-1,p+1]} = \left(\begin{smallmatrix} a_3 & 1 & 0 \\ a_2 & 0 & a_1 \end{smallmatrix}\right)$ for some $a_1, a_2, a_3 \in \mathcal{A}$. By the step-size assumption we have $a_1 \in C_0 \cup C_\pi$, and since $x^m_{p+1} = 0$ we have $a_1 \in \{0, \mathfrak{a}\}$. Therefore, $x^m_p = 1$ requires $a_2 \in E$, and by the step-size assumption $a_2 = 1$. Hence, $x^{m-1}_{p-1,p} = (1, 0)$. The claim follows by induction, and by spatial reflection symmetry. □

LEMMA 4.24. *If $x \in \Omega$ and there exist $p \in \mathbb{Z}$, $m \in \mathbb{N}_0$ such that $x^k_p = 0$ for all $k \geqslant m$, then $x^m \in Z$.*

Proof. Without loss of generality, suppose $x^k_p = 0$ for all $k \geqslant 0$. By induction over the position,

$$\text{for all } q \in \mathbb{Z} \text{ there exists } n = n(q) \geqslant 0 : x^k_q = 0 \quad \text{for all } k \geqslant n, \tag{17}$$

since otherwise $x^k_p \neq 0$ for some $k \geqslant 0$.

Suppose x is not the zero configuration (which would already mean $x \in Z$), and let $q_{\min} \in \mathbb{Z}$ be the nearest position to p such that $x_q \neq 0$. Without loss of generality, assume $q_{\min} > p$. Then $x^k_q = 0$ for all $p \leqslant q < q_{\min}$ and all $k \geqslant 0$. Consequently, $s_{q_{\min}-1}(x) = a \in R$ and there exists a change in the step size, $s^1_{q_{\min}-1}(x) = a + 1 \neq a$. Hence, $s_q(x) \in C_0 \cup C_\pi$ for all $q \in \mathbb{Z}$ by Lemma 4.22. However, by (17), for each step size $s_q(x) \in C_\pi$

https://doi.org/10.1017/etds.2020.18 Published online by Cambridge University Press

there exists some $k \geqslant n(q)$ such that $s_q^k(x) \notin C_\pi$, contradicting $x \in \Omega$. Hence, $s_q(x) \in C_0$ for all $q \in \mathbb{Z}$ which, together with $x \in \Omega$, implies $x \in Z$ by Lemma 4.21. □

4.3.1. *Constant step size.*

LEMMA 4.25. *Let $x \in \Omega \setminus Z$ with $s_p^m(x) = s_p^0(x)$ for all $m \in \mathbb{N}$ and some fixed $p \in \mathbb{Z}$. Then*

$$x \in \Omega_{\text{const}} := \{x \in \Omega \setminus Z \mid \textit{for all } q \in \mathbb{Z},\, m \in \mathbb{N} : s_q^m(x) = s_q^0(x)\}.$$

Moreover, $x \in X \setminus Z$ is $(\mathfrak{a}+1)$-periodic if and only if $x \in \Omega_{\text{const}}$.

Proof. Suppose $x \in \Omega$ and there exists some $p \in \mathbb{Z}$ such that $s_p^m(x) = c \in C_j$ for all $m \in \mathbb{N}_0$. By Lemma 4.8, for any $m \in \mathbb{N}$, there are two possibilities for constant step-size dynamics:

(1) $x_p^{[m,m+1]} \neq (0,0)^\intercal \neq x_{p+1}^{[m,m+1]}$ for all $m \in \mathbb{N}_0$l,

(2) $x_p^{[m,m+1]} = (0,0)^\intercal = x_{p+1}^{[m,m+1]}$ for some $m \in \mathbb{N}_0$.

Case (1). By Lemma 4.22 applied to $p \pm 1$, any step-size change of $s_{p-1}(x)$ or $s_{p+1}(x)$ implies a block $x_p^{[m,m+1]} = (0,0)^\intercal$ for some $m \in \mathbb{N}$, which does not occur in case (1). By induction over $q \in \mathbb{Z}$, $s_q^m(x)$ is constant for all $m \in \mathbb{N}_0$ and $q \in \mathbb{Z}$. In particular, x is $(\mathfrak{a}+1)$-periodic due to the absence of any zero block 0_ℓ, $\ell \geqslant 2$, in $(x_q^m)_{m\in\mathbb{N}}$ for any q.

Case (2). We show that in this case $x \in Z$ so that $x \notin \Omega_{\text{const}}$. The constant step size is $c = 0 \in C_0$, that is, $x_p^k = x_{p+1}^k$ for all $k \in \mathbb{N}_0$.

First, assume that $x_{[p,p+1]}^{m'} = (0,0)$ for all $m' \geqslant m$. By Lemma 4.24, $x^m \in Z$, that is, $s_p(x^m) \in C_0$ for all $p \in \mathbb{Z}$ and hence $s_p(x) \in C_0$ for all $p \in \mathbb{Z}$, meaning that $x \in Z$ (Lemma 4.21).

Next, suppose there exists some (smallest) $m' > m+1$ with $x_{[p,p+1]}^{m'} = (1,1)$, that is, there is a window

$$x_{[p-1,p+1]}^{[m'-2,m']} = \begin{pmatrix} a_3 & 1 & 1 \\ a_2 & 0 & 0 \\ a_1 & 0 & 0 \end{pmatrix} \tag{18}$$

for some $a_1, a_2, a_3 \in \mathcal{A}$. Since $x_p^{m'} = 1$ and $x_{p+1}^{m'-1} = 0$, we must have $a_2 \in E$ and $x_p^{m'-1} = 0$ implies $a_2 = 1$ so that $a_1 = 0$. This means $s_{p-1}^{m'-2}(x) \neq s_{p-1}^{m'-1}(x)$ so that, by Lemma 4.22, we know $s_q^k(x) \in C_0 \cup C_\pi$ for all $q \in \mathbb{Z}$ and $k \in \mathbb{N}_0$. By Lemma 4.23, the block $x_{[p-1,p]}^{m'-1} = (1,0)$ shifts back spatially to $x_{[p-m'-2,p-m'-1]} = (1,0)$. Hence, we can conclude that $s_q(x) \in C_0$ for all $p - m' - 2 \leqslant q \leqslant p$.

To conclude that $s_q(x) \in C_0$ for all $q \in \mathbb{Z}$, note that we can assume that there are infinitely many $k > m'$ with $x_{[p-1,p+1]}^{[k,k+1]} = \left(\begin{smallmatrix} a_1 & 1 & 1 \\ a_2 & 0 & 0 \end{smallmatrix}\right)$; otherwise we are again in the situation of Lemma 4.24. Since we have already concluded that all step sizes lie in $C_0 \cup C_\pi$, we must have $a_2 = 1$ and $a_1 = 2$ and, again by Lemma 4.22, the block $x_{[p-1,p]}^k = (1,0)$ shifts back to $x_{[p-1-k,p-k]} = (1,0)$. Since this holds for infinitely many increasing $k > m'$, one deduces $s_q(x) \in C_0$ for all $q \leqslant p$. By symmetry, also $s_q(x) \in C_0$ for $q > p$, that is, $x \in Z$ by Lemma 4.21. □

Remark 4.26. By reverse conclusion, any non-wandering point in $\Omega \setminus Z$ with some varying step size has nowhere constant step size. Lemma 4.25 shows in particular that Ω_{const} is a T-invariant subset of Ω.

4.3.2. *Varying step size.* Next, we let $x \in \Omega \setminus Z$ and suppose that for some position $p \in \mathbb{Z}$ the step size varies (i.e., $\exists m \in \mathbb{N} : s_p^m(x) \neq s_p^0(x) = c$). By the previous section, this implies $x \in \Omega_{\text{const}}^C$ and it turns out that $x \in \Omega_{\text{const}}^C \setminus Z$ is the following set:

$$\Omega_{\text{var}} := \bigcup_{p\in\mathbb{Z}} \{x \in \Omega \setminus \Omega_{\text{const}} : s_p^0(x) \in C_\pi,\ x_{[-\infty,p]} \in S_{\text{R},p,-}^{\#C_\pi},\ x_{[p+1,+\infty]} \in S_{\text{L},p+1,+}^{\#C_\pi}\},$$

$$S_{\text{L},p,+}^k := \{x \in S_{\text{L},p}^+ :\ \text{at most } k \text{ consecutive zeros occur in } x\},$$

$$S_{\text{R},p,-}^k := \{x \in S_{\text{R},p}^- :\ \text{at most } k \text{ consecutive zeros occur in } x\},$$

for $k \in \mathbb{N}_0$.

LEMMA 4.27. *If, for $x \in \Omega \setminus Z$, there exist $p \in \mathbb{Z}$ and $m \in \mathbb{N}$ such that $s_p^m(x) \neq s_p^0(x)$, then $x \in \Omega_{\text{var}}$ and $r > e + 1$.*

Proof. Recall that the only two options for varying step sizes are $c \in C_0$ and, if $r > e + 1$, $c \in C_\pi$ as for $r = e + 1$ we have $C_\pi = \{e + 1\}$, which does not allow for step-size variation. Hence, $\Omega_{\text{var}} = \varnothing$ for $r \leqslant e + 1$.

Since x is not identically zero, there must be a window

$$x_{[q,q+1]}^{[k,k+1]} \in \left\{ \begin{pmatrix} 1 & a+1 \\ 0 & a \end{pmatrix}, \begin{pmatrix} a+1 & 1 \\ a & 0 \end{pmatrix} \right\}.$$

If $a \in E \neq 1$ we have $s_q^k(x) \in \mathcal{A} \setminus (C_0 \cup C_\pi)$, but by Lemma 4.22 we have that $s_q^0(x) \in C_0 \cup C_\pi$ for all $q \in \mathbb{Z}$. Therefore $a = 1$ and, as in the proof of Lemma 4.25, by backtracking excitation loops in time it follows that $x_{[-\infty,p]} \in S_{\text{R},p}^-$ and $x_{[p+1,+\infty]} \in S_{\text{L},p+1}^+$. If $s_q^0(x) \in C_0$ for all $q \in \mathbb{Z}$ then $x \in Z$, that is, $x \notin \Omega_{\text{var}}$. Therefore, there is $q \in \mathbb{Z}$ with $s_q^0(x) \in C_\pi$.

In this case, we can backtrack analogously to Lemma 4.25; however, the restriction $2 \leqslant \ell \leqslant \#C_\pi$ on zero blocks 0_ℓ occurring in $(x_q^m(0))_{m\in\mathbb{N}}$ (cf. Corollary 4.17) implies that at most $\#C_\pi$ consecutive zeros can occur in x, that is, $x_{[p+1,+\infty]} \in S_{\text{L},p+1,+}^{\#C_\pi}$ and $x_{[-\infty,p]} \in S_{\text{R},p,-}^{\#C_\pi}$, hence $x \in \Omega_{\text{var}}$. □

Using the fact that $C_\pi = \varnothing$ for $e + 1 > r$, which means $\Omega_{\text{var}} = \varnothing$, the lemmas together prove Theorem 4.5 in particular.

4.4. *Computing the topological entropy: proof of Theorem 4.6.* In this section we finally determine the topological entropy $h(X, T)$ of T using $h(X, T) = h(\Omega, T|_\Omega)$.

By Theorem 4.5, the non-wandering set is the union of disjoint T-invariant sets, $\Omega = Z \uplus \Omega_{\text{const}} \uplus \Omega_{\text{var}}$, so that

$$h(\Omega, T|_\Omega) = \max\{h(Z, T|_Z), h(\Omega_{\text{const}}, T|_{\Omega_{\text{const}}}), h(\Omega_{\text{var}}, T|_{\Omega_{\text{var}}})\}. \tag{19}$$

By Proposition 3.5, $h(Z, T|_Z) = 2 \ln \rho_{\mathfrak{a}}$ and it remains to consider $h(\Omega_{\text{const}}, T|_{\Omega_{\text{const}}})$ and $h(\Omega_{\text{var}}, T|_{\Omega_{\text{var}}})$.

https://doi.org/10.1017/etds.2020.18 Published online by Cambridge University Press

As to Ω_{const}, by Lemma 4.25 this set contains $(\mathfrak{a}+1)$-periodic configurations only, which directly implies

$$h(\Omega_{\mathrm{const}}, T|_{\Omega_{\mathrm{const}}}) = 0. \tag{20}$$

From Theorem 4.5 we also know that $\Omega_{\mathrm{var}} = \varnothing$ if and only if $r \leqslant e+1$ and hence we restrict ourselves in what follows to the case $r > e+1$. By Remark 4.14, $T|_{\Omega_{\mathrm{var}}}$ splits into two independent dynamics on the lattices to the left and right of the particular unique stationary dislocation $p \in \mathbb{Z}$ with step size $s_p^0(x) \in C_\pi$. As the position of the dislocation is stationary, we can make use of the skew-product structure established in §3.4 in order to find an upper estimate for $h(\Omega_{\mathrm{var}}, T|_{\Omega_{\mathrm{var}}})$. To this end, let

$$\begin{aligned} Q_0 &:= \{(x, y) \in S^{\#C_\pi}_{\mathrm{R},0,-} \times S^{\#C_\pi}_{\mathrm{L},1,+} : y_1 = x_0 + c,\, c \in C_\pi\} \subset \Sigma_- \times \Sigma_+, \\ W &:= Q_0 \times \mathbb{Z}, \\ V &:= \Omega_{\mathrm{var}} \times \mathbb{Z}. \end{aligned}$$

On V and W, respectively, consider the maps

$$\begin{aligned} f &:= T|_{\Omega_{\mathrm{var}}} \times \mathrm{id} \colon V \to V, \\ g &:= (\sigma_{\mathrm{R},-} \times \sigma_{\mathrm{L},+}) \times \mathrm{id} \colon W \to W. \end{aligned}$$

For $x \in \Omega_{\mathrm{var}}$, let $p(x) \in \mathbb{Z}$ denote its unique stationary separating position (dislocation) with step size $s^0_{p(x)}(x) \in C_\pi$. We define $\varphi\colon V \to W$ by

$$\varphi((x, p(x))) := (x_{[-\infty, p(x)]}, x_{[p(x)+1, +\infty]}, p(x)).$$

(V, f) and (W, g) are topologically conjugate, that is, the diagram

$$\begin{array}{ccc} V & \xrightarrow{\ f\ } & V \\ {\scriptstyle\varphi}\downarrow & & \downarrow{\scriptstyle\varphi} \\ W & \xrightarrow{\ g\ } & W \end{array}$$

commutes, $\varphi \circ f = g \circ \varphi$, where φ is a homeomorphism. Thus, $h(V, f) = h(W, g)$. Since the identity map has zero topological entropy,

$$h(\Omega_{\mathrm{var}}, T|_{\Omega_{\mathrm{var}}}) = h(V, f) = h(W, g) = h(Q_0, \sigma_{\mathrm{R},-} \times \sigma_{\mathrm{L},+}).$$

Note that $Q_0 \subset \Sigma_- \times \Sigma_+$ is an invariant (proper) subset with respect to the product map $\sigma_{\mathrm{R},-} \times \sigma_{\mathrm{L},+}$. Using the product rule of topological entropy,

$$\begin{aligned} h(Q_0, \sigma_{\mathrm{R},-} \times \sigma_{\mathrm{L},+}) &\leqslant h(\Sigma_- \times \Sigma_+, \sigma_{\mathrm{R},-} \times \sigma_{\mathrm{L},+}) \\ &= h(\Sigma_-, \sigma_{\mathrm{R},-}) + h(\Sigma_+, \sigma_{\mathrm{L},+}) = 2 \ln \rho_{\mathfrak{a}}. \end{aligned}$$

In fact, we next show that the upper bound is strictly smaller than $2 \ln \rho_{\mathfrak{a}}$. In preparation, note that Q_0 is a $(\sigma_{\mathrm{R},-} \times \sigma_{\mathrm{L},+})$-invariant subset of $S^{\#C_\pi}_{\mathrm{R},0,-} \times S^{\#C_\pi}_{\mathrm{L},1,+}$, that is,

$$\begin{aligned} h(Q_0, \sigma_{\mathrm{R},-} \times \sigma_{\mathrm{L},+}) &\leqslant h(S^{\#C_\pi}_{\mathrm{R},0,-} \times S^{\#C_\pi}_{\mathrm{L},1,+}, \sigma_{\mathrm{R},-} \times \sigma_{\mathrm{L},+}) \\ &= h(S^{\#C_\pi}_{\mathrm{R},0,-}, \sigma_{\mathrm{R},-}) + h(S^{\#C_\pi}_{\mathrm{L},1,+}, \sigma_{\mathrm{L},+}). \end{aligned}$$

https://doi.org/10.1017/etds.2020.18 Published online by Cambridge University Press

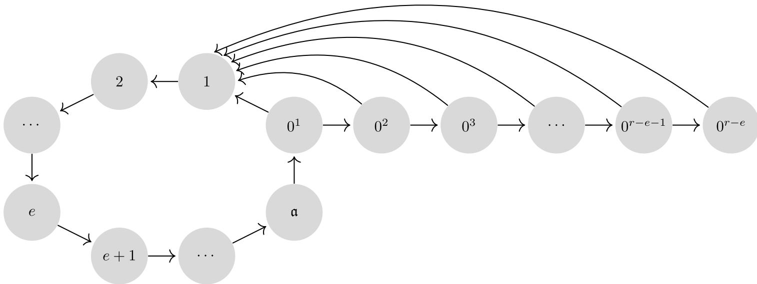

FIGURE 12. Transition graph for the one-sided subshifts $S^{\#C_\pi}_{\mathrm{R},p,-}$ and $S^{\#C_\pi}_{\mathrm{L},p,+}$.

The topological entropies on the right-hand side of the equation can be computed by considering semi-infinite walks on the graph corresponding to the alphabet

$$\mathcal{A}' := (\mathcal{A} \setminus \{0\}) \cup \{0^i : 1 \leqslant i \leqslant \#C_\pi\}$$

and the dynamics resulting from replacing the trivial transition $0 \to 0$ in Figure 2 by transitions

$$0^i \to 1 \quad \text{for all } 1 \leqslant i \leqslant \#C_\pi,$$
$$0^i \to 0^j \quad \text{exactly if } 1 \leqslant i,\ j \leqslant \#C_\pi \text{ and } j = i + 1;$$

cf. Figure 12. The resulting transition matrix $M \in \{0, 1\}^{2r\times 2r}$ is of block form

$$M = \begin{pmatrix} A & B \\ C & D \end{pmatrix}$$

with quadratic matrices $A \in \{0, 1\}^{(\#C_\pi)^2}$ and $D \in \{0, 1\}^{(\mathfrak{a})^2}$ with 1s on the upper off-diagonal and 0s elsewhere. The matrix $B \in \{0, 1\}^{\#C_\pi\times\mathfrak{a}}$ is composed of the first column $(1, 1, \ldots, 1)^\intercal$ and 0s elsewhere. Finally, the matrix $C \in \{0, 1\}^{\mathfrak{a}\times\#C_\pi}$ has a 1 in the last entry of the first column (which corresponds to the edge $\mathfrak{a} \to 0^1$) and 0s elsewhere.

In order to determine the characteristic polynomial of M, let I denote the unit matrix of suitable dimension and note that $D - \lambda I$ is invertible for $\lambda \neq 0$; its inverse matrix is given by

$$(D - \lambda I)^{-1} = -\begin{pmatrix} \lambda^{-1} & \lambda^{-2} & \lambda^{-3} & \ldots & \ldots & \lambda^{-\mathfrak{a}} \\ & \lambda^{-1} & \lambda^{-2} & \lambda^{-3} & \ldots & \lambda^{-(\mathfrak{a}-1)} \\ & & \ddots & \ddots & \ddots & \vdots \\ & & & \ddots & \ddots & \lambda^{-3} \\ & & & & & \lambda^{-2} \\ & & & & & \lambda^{-1} \end{pmatrix}, \tag{21}$$

where blank entries are 0s. The product of $(D - \lambda I)^{-1}$ and C is an $(\mathfrak{a}) \times \#C_\pi$-matrix whose first column is given by the last column of (21) and is 0 otherwise. Multiplying by matrix B gives the $\#C_\pi \times \#C_\pi$-matrix $Q := B(D - \lambda I)^{-1}C$ whose first column is given

https://doi.org/10.1017/etds.2020.18 Published online by Cambridge University Press

by $-(\lambda^{-\mathfrak{a}}, \ldots, \lambda^{-\mathfrak{a}})^\intercal$ and is 0 otherwise. Subtracting Q from $A - \lambda I$ yields

$$P := (A - \lambda I) - Q = \begin{pmatrix} -\lambda + \lambda^{-\mathfrak{a}} & 1 & & & & \\ \lambda^{-\mathfrak{a}} & -\lambda & 1 & & & \\ \lambda^{-\mathfrak{a}} & & -\lambda & 1 & & \\ \vdots & & & \ddots & \ddots & \\ \lambda^{-\mathfrak{a}} & & & & -\lambda & 1 \\ \lambda^{-\mathfrak{a}} & & & & & -\lambda \end{pmatrix}$$

whose determinant can be computed by expanding along the first row. By $\#C_\pi = r - e$,

$$|P| = \lambda^{-\mathfrak{a}}(\lambda^{2r} - \lambda^{r-e-1}) - \begin{vmatrix} \lambda^{-\mathfrak{a}} & 1 & 0 & \ldots & 0 \\ \vdots & -\lambda & 1 & \ldots & 0 \\ \vdots & 0 & -\lambda & \ddots & \\ \lambda^{-\mathfrak{a}} & & & \ddots & 1 \\ \lambda^{-\mathfrak{a}} & & & & -\lambda \end{vmatrix}. \tag{22}$$

The determinant on the right-hand side of (22) can be computed again by expanding along the first row, yielding the summand $\lambda^{-\mathfrak{a}}(-\lambda)^{r-e-2}$ and another determinant computable by expanding along the first row. Repeating this until we end up with the summand $\lambda^{-\mathfrak{a}}$, the determinant of P is eventually given by

$$|P| = \lambda^{-\mathfrak{a}} \cdot \bigg(\lambda^{2r} - \sum_{i=0}^{\#C_\pi - 1} \lambda^i\bigg).$$

Using $|D - \lambda I| = (-\lambda)^{\mathfrak{a}}$ and the determinant formula for block matrices,

$$\begin{aligned} |M - \lambda I| = |D - \lambda I| \cdot |P| &= (-\lambda)^{\mathfrak{a}} \lambda^{-\mathfrak{a}} \bigg(\lambda^{2r} - \sum_{i=0}^{\#C_\pi - 1} \lambda^i\bigg) \\ &= (-1)^{\mathfrak{a}} \bigg(\lambda^{2r} - \sum_{i=0}^{r-e-1} \lambda^i\bigg). \end{aligned}$$

Since we are interested in the roots of this polynomial, we can neglect the factor $(-1)^{\mathfrak{a}}$ and consider the polynomial

$$g_{e,r}(\lambda) = \lambda^{2r} - \sum_{i=0}^{r-e-1} \lambda^i$$

which has exactly one positive (simple) root $\eta_{e,r}$ by Descartes' rule, and $\eta_{e,r} > 1$ since $g_{e,r}(0), g_{e,r}(1) < 0$ and the leading coefficient is positive. Hence,

$$h(S^{\#C_\pi}_{\mathrm{R},0,-}, \sigma_{\mathrm{R},-}) = h(S^{\#C_\pi}_{\mathrm{L},1,+}, \sigma_{\mathrm{L},+}) = \ln \eta_{e,r}. \tag{23}$$

Finally, we show $\eta_{e,r} < \rho_{\mathfrak{a}}$ and hence $h(\Omega_{\mathrm{var}}, T|_{\Omega_{\mathrm{var}}}) < 2\ln(\rho_{\mathfrak{a}})$. First note that $g_{e,r}(\lambda) = \lambda^{2r} - (\lambda^{r-e} - 1)/(\lambda - 1) = \lambda^{r-e} f_c(\lambda) + 1$, where f_c is the polynomial from Lemma 3.7 with unique positive root ρ_c. Consequently, $g_{e,r}(\rho_c) = 1 > 0$. This implies $\eta_{e,r} < \rho_{\mathfrak{a}}$ since the root $\eta_{e,r} > 1$ of $g_{e,r}$ is unique and its leading coefficient is positive,

https://doi.org/10.1017/etds.2020.18 Published online by Cambridge University Press

so that $g_{e,r}(\lambda) > 0$, $\lambda > 0 \Rightarrow \lambda > \eta_{e,r}$. In particular, $1 < \eta_{e,r} < \rho_c$, that is, $\eta_{e,r} \to 1$ as $e \to \infty$ by Lemma 3.7. This concludes the proof of Theorem 4.6.

Recall that the topological entropy $h(Z, T_{|Z})$ depends on e, r only through $\mathfrak{a}$; cf. Lemma 3.7. We end this section by commenting on scaling bounds of (23).

Remark 4.28. The asymptotic scaling of (23) and, consequently, of the upper bound $2 \ln \eta_{e,r}$ of $h(\Omega_{\text{var}}, T_{|\Omega_{\text{var}}})$ differs from the scaling of $2 \ln(\rho_{\mathfrak{a}}) = h(Z, T_{|Z})$, and in particular depends on the difference $r - e$.

More specifically, we next show that if $r - e$ is constant then $\zeta := \eta_{e,r} - 1 \sim 1/r$ as $r \to \infty$, which is thus asymptotically smaller than $\rho_{\mathfrak{a}} \sim (\ln(\mathfrak{a}))/\mathfrak{a}$; recall $0 < \zeta < (\ln \mathfrak{a})/\mathfrak{a}$ so $\zeta \to 0$ as $\mathfrak{a} \to \infty$. In particular, a time-rescaled topological entropy on Ω_{var} as in Corollary 3.8 behaves differently than that on Z.

As to the proof, we rewrite $g_{e,r}(1 + \zeta) = 0$ and take logarithms as follows:

$$(1+\zeta)^{r-e} = 1 + \zeta(1+\zeta)^{2r} \Leftrightarrow (r-e)\ln(1+\zeta) = \ln(1+\zeta(1+\zeta)^{2r})$$
$$\Leftrightarrow (r-e) = \frac{\ln(1+\zeta(1+\zeta)^{2r})}{\ln(1+\zeta)}.$$

Hence, if $r - e$ is constant then, as $r \to \infty$, we have $\zeta(1+\zeta)^{2r} \sim \zeta$, that is, $(1+\zeta)^{2r} \sim 1$ and therefore $\zeta \sim 1/r$.

In contrast, if e is constant one can show that $\eta \sim (\ln r)/r$, that is, the upper bound $\ln(\eta)$ for the topological entropy on Ω_{var} scales as that on Z. However, we omit this as we do not investigate a lower bound here.

Acknowledgements. We thank the reviewer for careful reading and helpful comments. This work has been supported by DFG grant RA 2788/1-1.

REFERENCES

[1] R. L. Adler, A. G. Konheim and M. H. McAndrew. Topological entropy. *Trans. Amer. Math. Soc.* **114**(2) (1965), 309–319.

[2] F. Blanchard, P. Kurka and A. Maass. Topological and measure-theoretic properties of one-dimensional cellular automata. *Phys. D* **103**(1) (1997), 86–99.

[3] R. Bowen. Entropy for group endomorphisms and homogeneous spaces. *Trans. Amer. Math. Soc.* **153** (1971), 401–414.

[4] E. I. Dinaburg. A correlation between topological entropy and metric entropy. *Dokl. Akad. Nauk SSSR* **190** (1970), 19–22.

[5] R. Durrett and J. E. Steif. Some rigorous results for the Greenberg–Hastings model. *J. Theoret. Probab.* **4**(4) (1991), 669–690.

[6] J. M. Greenberg, B. D. Hassard and S. P. Hastings. Pattern formation and periodic structures in systems modeled by reaction–diffusion equations. *Bull. Amer. Math. Soc.* **84**(6) (1978), 1296–1327.

[7] B. Hasselblatt, Z. Nitecki and J. Propp. Topological entropy for non-uniformly continuous maps. *Discrete Contin. Dyn. Syst. A* **22**(1&2) (2008), 201–213.

[8] L. P. Hurd, J. Kari and K. Culik. The topological entropy of cellular automata is uncomputable. *Ergod. Th. & Dynam. Sys.* **12**(2) (1992), 255–265.

[9] E. M. Izhikevich. *Dynamical Systems in Neuroscience: The Geometry of Excitability and Bursting*. MIT Press, Cambridge, MA, 2010.

[10] A. Katok and B. Hasselblatt. *Introduction to the Modern Theory of Dynamical Systems (Encyclopedia of Mathematics and its Applications)*. Cambridge University Press, Cambridge, 1997.

[**11**] V. Krinsky and H. Swinney. *Wave and Patterns in Biological and Chemical Excitable Media*. North-Holland, Amsterdam, 1991.
[**12**] D. Lind and B. Marcus. *An Introduction to Symbolic Dynamics and Coding*. Cambridge University Press, Cambridge, 1995.
[**13**] N. Manz and O. Steinbock. Propagation failures, breathing pulses, and backfiring in an excitable reaction–diffusion system. *Chaos* **16**(3) (2006).
[**14**] T. Meyerovitch. Finite entropy for multidimensional cellular automata. *Ergod. Th. & Dynam. Sys.* **28**(4) (2008), 1243–1260.
[**15**] J. E. Pearson. Complex patterns in a simple system. *Science* **261**(5118) (1993), 189–192.
[**16**] J.-J. Perraud, A. De Wit, E. Dulos, P. De Kepper, G. Dewel and P. Borckmans. One-dimensional ‘spirals’: Novel asynchronous chemical wave sources. *Phys. Rev. Lett.* **71** (1993), 1272–1275.
[**17**] V. Petrov, S. K. Scott and K. Showalter. Excitability, wave reflection, and wave splitting in a cubic autocatalysis reaction–diffusion system. *Philos. Trans. Roy. Soc. Lond.* A **347** (1994), 631–642.
[**18**] W. N. Reynolds, J. E. Pearson and S. Ponce-Dawson. Dynamics of self-replicating patterns in reaction diffusion systems. *Phys. Rev. Lett.* **72**(17) (1994), 2797.
[**19**] D. Ulbrich. Dynamics of the 1D Greenberg–Hastings cellular automaton. *Master’s thesis*, Universität Bremen, 2016, supervised by J. D. M. Rademacher and T. Samuel.
[**20**] P. Walters. *An Introduction to Ergodic Theory (Graduate Texts in Mathematics, 79)*. Springer, New York, 2000.
[**21**] W. Yangeng, G. Wei and W. H. Campbell. Sensitive dependence on initial conditions between dynamical systems and their induced hyperspace dynamical systems. *Topol. Appl.* **156**(4) (2009), 803–811.